Alternatively activated macrophages are not an appreciable source of catecholamines and do not contribute to adipose tissue adaptive thermogenesis

Katrin Fischer[1,2], Henry H. Ruiz[3], Kevin Jhun[3], Brian Finan[1,2], Verena van der Heide[3], Anastasia V. Kalinovich[4], Natasa Petrovic[4], Yochai Wolf[5], Christoffer Clemmensen[1,2], Andrew C. Shin[3,6], Senad Divanovic[7], Frank Brombacher[8], Elke Glasmacher[1], Susanne Keipert[1], Martin Jastroch[1,9], Joachim Nagler[10], Karl-Werner Schramm[10], Dasa Medrikova[11], Gustav Collden[1,2], Stephen C. Woods[12], Stephan Herzig[11], Dirk Homann[3], Steffen Jung[5], Jan Nedergaard[4], Barbara Cannon[4], Matthias H. Tschöp[1,2], Timo D. Müller[1,#,*], Christoph Buettner[3,13#,*]

[1]Institute for Diabetes and Obesity, Helmholtz Diabetes Center (HDC), Helmholtz Zentrum München and German National Diabetes Center (DZD), 85764 Neuherberg, Germany. [2]Division of Metabolic Diseases, Department of Medicine, Technische Universität München, 80333 Munich, Germany. [3]Diabetes, Metabolism and Obesity Institute, Icahn School of Medicine at Mount Sinai, NY 10029, USA. [4]Department of Molecular Biosciences, The Wenner-Gren Institute, Stockholm University, 10691 Stockholm, Sweden. [5]Weizmann Institute of Science Department of Immunology, 76100 Rehovot, Israel. [6]Department of Nutritional Sciences, College of Human Sciences, Texas Tech University, Lubbock, TX 79423, USA. [7]Department of Pediatrics, Division of Immunobiology, Cincinnati Children's Hospital Medical Center, OH 45229 Cincinnati, USA. [8]International Center for Genetic Engineering and Biotechnology, Cape Town component & University of Cape Town, IDM, Division Immunology & SAMRC, South Africa. [9]Department of Animal Physiology, Faculty of Biology, Philipps University of Marburg, 35032 Marburg, Germany. [10]Molecular Exposomics, Helmholtz Zentrum München, German National Diabetes Center (DZD), 85764 Neuherberg, Germany. [11]Institute for Diabetes and Cancer (IDC), Helmholtz Zentrum München, German National Diabetes Center (DZD), 85764 Neuherberg, Germany, and Joint IDC-Heidelberg Translational Diabetes Program, Inner Medicine I, Heidelberg University Hospital, 69120 Heidelberg, Germany. [12]Metabolic Diseases Institute, Department of Psychiatry and Behavioral Neuroscience, University of Cincinnati, OH 45237 Cincinnati, USA. [13]Department of Medicine, Icahn School of Medicine at Mount Sinai, NY 10029, USA.

*these authors contributed equally

[#]Corresponding authors/Lead contact:

Timo D. Müller, Institute for Diabetes and Obesity, Helmholtz Zentrum München, German Research Center for Environmental Health (GmbH), Neuherberg, Germany; timo.mueller@helmholtz-

muenchen.de and Christoph Buettner, Icahn School of Medicine at Mount Sinai, New York, USA; christoph.buettner@mssm.edu

Keywords: Macrophages, catecholamine, tyrosine hydroxylase, thermogenesis, Ucp1, lipolysis

Abstract

Adaptive thermogenesis is under the control of the sympathetic nervous system whose chief effector is norepinephrine (NE). Recent studies reported that alternatively activated macrophages express tyrosine hydroxylase (TH) to provide an alternative source of locally secreted catecholamines that enhance thermogenesis by activating brown adipose tissue and by "browning" white adipose tissue. We here report that the deletion of *TH* in hematopoetic cells of adult mice neither alters energy expenditure upon cold exposure nor stimulates browning in inguinal adipose tissue. Bone marrow-derived macrophages did not release NE in response to stimulation with Interleukin-4 (IL-4), and conditioned media from IL-4 stimulated macrophages failed to induce expression of thermogenic genes, such as the one for uncoupling protein 1 (*Ucp1*). Chronic IL-4 treatment failed to modify energy expenditure in WT, *Ucp1*$^{-/-}$ and *Il4ra*$^{-/-}$ mice. Consistent with these findings, adipose tissue-resident macrophages did not express TH, the essential enzyme in catecholamine synthesis. Thus, we conclude that alternatively activated macrophages do not synthesize relevant amounts of catecholamines and hence are not likely to play a direct role in adipocyte metabolism or adaptive thermogenesis.

Introduction

Thermogenesis is critical for the survival of endothermic mammals and birds as it allows for maintaining a stable body temperature even in a cold environment[1,2]. Death from hypothermia has remained a major cause of mortality throughout evolution. Hence the need for efficient thermogenesis represents an evolutionary pressure that has shaped the biology of all endothermic homeotherms[3]. Regulation of body temperature also plays a central role in energy homeostasis, and pharmacological stimulation of energy expenditure is considered a valuable strategy to combat obesity and its co-morbidities[4]. Detailed understanding of the physiological and molecular underpinnings regulating adaptive thermogenesis is therefore of utmost importance. It is well established that catecholamines are a key driver of thermogenesis by uncoupling respiration and/or inducing futile cycling in brown adipose tissue (BAT) and brite white adipose tissue (WAT). Notably, catecholamines are also key for the induction of lipolysis in WAT that prompts the release of fatty acids, the principal substrate for BAT thermogenesis[5]. In the periphery, catecholamines are classically believed to originate from either sympathetic post-ganglionic neurons or else the adrenal medulla. Challenging this traditional view, recent reports proposed a major paradigm shift by suggesting that alternatively activated macrophages are another important source of catecholamines, and that they consequently represent a previously overlooked mechanism to adjust thermogenesis. In that model, cold exposure enhances alternative activation of macrophages, thereby inducing TH and resulting in the production and secretion of NE to enhance non-shivering thermogenesis in BAT, lipolysis in WAT[6] and browning of inguinal WAT (iWAT)[7]. Most *in vivo* data upon which this concept rests are based on the analysis of mice with a life-long deficiency of key 'M2 signaling nodes': i.e., IL-

4/13, Il4ra, Stat6, Il4ra$^{f/f}$Lyz2^{Cre}, and TH$^{f/f}$Lyz2^{Cre} mice. Notably, all of these germline knockout (KO) models share the caveat that their metabolic phenotype can be compromised through developmental processes, and/or, through altered sympathetic regulation, since all of these genes are also expressed in the nervous system. Accordingly, the aim of these studies was to assess the role of macrophages in mice with adult-onset peripheral deletion of *TH*, as well as, to further evaluate the role of alternatively activated macrophages in regulating white, brown and brite adipocyte function *in vitro* and *in vivo*. Collectively we show here, using a combination *in vivo* and *in vitro* approaches that alternatively activated macrophages do not synthesize sufficient amounts of catecholamines and are thus unlikely to play a direct role in adipocyte metabolism or adaptive thermogenesis.

Results

Peripheral catecholamines play a critical role in thermogenesis

Lifelong deletion of *TH* results in early embryonic lethality, possibly due to the important role of catecholamines in the central nervous system (CNS) during development[8]. To study the role of peripheral catecholamines in thermoregulation, we generated mice, in which *TH* deletion is induced in all peripheral tissues of adult mice including the sympathetic nervous system (SNS) and hematological cells, but not in the CNS (Fig. 1a; herein called "THΔper mice"). Ablation of TH protein in peripheral tissues (BAT, spleen, liver and epididymal white adipose tissue (eWAT)) after tamoxifen administration was confirmed by Western blot analysis (Fig. 1b), and resulted in the marked depletion of NE levels in all peripheral tissues analyzed as compared to wild-type (WT) controls (Fig. 1c). In line with the prediction that THΔper mice have reduced sympathetic activity relative to WT controls, the animals exhibited impaired thermoregulation when exposed to 4°C (Fig. 1d), which is consistent with a key role of catecholamines in thermogenesis. We also used tissue extracts from these mice to validate several commercially available antibodies against TH, several of which had a strong non-specific band of similar molecular size as TH, raising the concern that without appropriate controls, it is difficult to ascertain the specificity of any of these antibodies in applications such as Western blot (Fig. S1).

To probe if catecholamines produced by alternatively activated macrophages play a relevant role in thermoregulation, we generated bone marrow-chimeric mice where *TH* is specifically deleted from hematopoetic cells (including macrophages) in an inducible manner. We first transplanted bone marrow from WT and non-induced THΔper mice into irradiated WT recipient mice. Fluorescence-activated cell sorting

(FACS) analysis conducted on peripheral blood ~8 weeks later revealed a >90% reconstitution with lymphocytes and granulocytes of WT or THΔper donor origin in the majority of chimeras (Fig. 2a). Subsequent tamoxifen treatment of the chimeras resulted in *TH* ablation from hematopoetic cells (including macrophages) in THΔper, but not WT chimeras without affecting body weight (Fig. 2b). Notably, energy expenditure did not differ between THΔper chimera mice and their WT controls at room temperature (21°C) and after exposure to cold by successively lowering temperatures to 15°C, 10°C and 6°C (Fig. 2c,d). Furthermore, locomotor activity (Fig 2e), substrate utilization, as assessed by the respiratory exchange ratio (RER) (Fig. 2f), and body core temperature (Fig. 2g) were not different. Consistent with the observation that energy expenditure and core body temperature are not changed after *TH* deletion in hematologic cells, THΔper chimera also exhibited a comparable cold-induced increase in iWAT *Ucp1* mRNA levels to that seen in WT controls (Fig. 2h).

Macrophages do not affect differentiation or browning of inguinal white adipocytes

To evaluate a possible role of macrophages in adipocyte metabolism *in vitro*, we isolated pre-adipocytes from iWAT, depleted the macrophages by magnetic bead-mediated sorting of CD11b-positive cells, cultured and differentiated them *in vitro* (henceforth described as “primary cells”). We confirmed successful macrophage depletion by the lack of *Itgam* (alias *CD11b*) and *Adgre1* mRNA levels during adipocyte differentiation (Fig. S2a,b) and absence of M1 and M2 markers (*Tnf, Arg1, Mgl2, Mrc1* and *Il10*) in fully differentiated iWAT primary cells (Fig. S2c,d). Lipid accumulation, assessed by Oil Red O staining, was not affected by the absence of macrophages (Fig. S2e,f), indicating that macrophages are dispensable for adipocyte

differentiation. Consistent with this notion, expression profiles of markers indicative of adipocyte differentiation (*Fasn*, *Adipoq*, *Fabp4*, *Pparg*) were not affected by the absence of macrophages (Fig. S3a-d). Likewise, we observed no changes for gene programs indicative of fatty acid synthesis, fatty acid transport, cytokine signaling, lipoprotein metabolism, carbohydrate metabolism, lipogenesis or lipolysis (Fig. S3e-j). Further, we observed no differences in the expression profile of genes related to mitochondrial electron transport (*Cycs, Cox4i1*) (Fig. S2g,h) or of key thermogenic genes (*Ucp1, Ppargc1a* (alias *Pgc-1α*) and *Prdm16*) during differentiation of iWAT primary cells (Fig. S2i-k). We next asked whether the depletion of macrophages impaired the ability of isoproterenol to stimulate expression of *Ucp1* and *Pgc-1α* in differentiated iWAT primary cells, and found no difference (Fig. S2l,m). Consistent with the observation that isoproterenol-induced stimulation of *Ucp1* and *Pgc-1α* are not affected by the absence of macrophages, we observed no changes in basal respiration, ATP-production, maximal respiration or non-mitochondrial respiration, as assessed by the oxygen consumption rate following treatment with isoproterenol, oligomycin, carbonyl cyanide-4-(trifluoromethoxy)phenylhydrazone (FCCP) or rotenone /antimycin A/2-deoxyglucose (Fig. S2n-p).

To probe whether macrophages first need to undergo polarization to stimulate thermogenesis, we treated bone marrow-derived macrophages (BMDMs) with various doses of IL-4 (5, 10, or 20 ng/ml), and then used the conditioned media (CM) to stimulate differentiated iWAT primary cells. IL-4 treatment robustly enhanced expression of the M2 markers *Arg1*, *Mrc1* and *Mgl2* in the BMDMs as compared to vehicle control (Fig. 3a-c). However, despite robust polarization, the CM failed to stimulate the expression of *Ucp1* or *Pgc-1α* in the differentiated iWAT primary cells (Fig. 3d,e). In summary, these data demonstrate that macrophages are neither

required for differentiation of iWAT primary adipocytes, nor likely to play a role in browning or β-adrenergic receptor-mediated stimulation of thermogenesis in these cells.

M2 macrophages do not affect thermogenesis in BAT primary cells

To evaluate the thermogenic effect of M2-activated macrophages in BAT, we used CM from IL-4-stimulated BMDMs to stimulate differentiated BAT primary cells. Despite robust M2 polarization of the BMDMs (Fig. 3a-c), we observed no effect of the CM on expression of *Ucp1* and *Pgc-1α* (Fig. 3f,g), congruent with the findings obtained with iWAT primary cells (Fig. 3d,e). IL-4-CM also failed to activate hormone-sensitive lipase (HSL) at both IL-4 doses tested (Fig. 3h,i) and independent of the duration of IL-4 treatment (15 min, 30 min, 1 h, 3 h or 6 h) (Fig. S4). Notably, we confirmed failure of M2 macrophages to induce thermogenic gene programs in iWAT and BAT primary cells in several independent experiments in primary cells obtained from both BALB/c (Fig. 3) and C57Bl/6J mice (data not shown), and also from primary cells stimulated with IL-4-CM from Raw264.7 cells (Fig. S5).

Failure of the IL-4 conditioned media to stimulate thermogenic gene programs in both iWAT and BAT primary cells prompted us to quantify IL-4-stimulated catecholamine production in BMDMs. Notably, despite robust IL-4 induction of M2 polarization (Fig. 3a-c), high performance liquid chromatography (HPLC) analysis revealed no stimulatory effect of IL-4 relative to vehicle control at any tested dose (5, 10, 20 ng/ml) on NE, epinephrine, 5-hydroxyindoleacetic acid, homovanillic acid, dopamine or 5-hydroxytryptamin (Fig. S6). Of note, IL-4 failed to induce catecholamine levels in both the supernatant (Fig. S6a-f), and within the macrophages themselves (Fig. S6g-l). These data suggest that M2 macrophages lack the ability to produce sufficient

catecholamines and induce thermogenic gene programs in iWAT or BAT primary cells.

Chronic IL-4 treatment has no effect on energy metabolism in WT, *Il4ra*$^{-/-}$ and *Ucp1*$^{-/-}$ mice

We next assessed if chronic IL-4 treatment in WT and *Il4ra*$^{-/-}$ mice exposed to various declining environmental temperatures (30°C, 20°C, 10°C, or 5°C) alters energy expenditure. Daily intraperitoneal administration of IL-4 (50 µg/kg) for 12 d did not alter body weight (Fig. 4a) or energy expenditure in WT or *Il4ra*$^{-/-}$ mice at any temperature tested (Fig. 4b,c). Notably, despite robust induction of M2 polarization in BAT (Fig. 4d-f) after IL-4 treatment – confirming that the IL-4 was fully functional – such treatment did not increase expression of *Ucp1* or *Pgc-1α* in BAT relative to controls (Fig. 4h,i). Mice lacking the Interleukin-4 receptor alpha (Il4ra) show no elevated expression *Arg1*, *Mrc1*, *Mgl2* after IL-4 treatment (Fig. 4d-f,i) and thus confirm their incapability to activate M2 type macrophages via Il4ra-mediated signaling.

Consistent with our *in vitro* data demonstrating no effect of IL-4 on phosphorylation of HSL (p-HSL) in iWAT and BAT primary cells (Fig. 3h,i; Fig. S4), we found no difference in p-HSL in mice chronically treated with IL-4 relative to controls (Fig. 4j-n). Supporting these data, HPLC analysis revealed no difference in levels of catecholamines including NE or their metabolites in cold-exposed mice treated chronically with IL-4 (Fig. 4o).

We next evaluated the metabolic effect of chronic IL-4 treatment in C57Bl/6 WT and *Ucp1*$^{-/-}$ mice housed at thermoneutrality (30°C) to assess a possible role of UCP1 in driving the reported effects of IL-4 on energy homeostasis. We administered IL-4 (50

µg/kg) daily for 8 d, following the final injection, we recorded energy expenditure at 30°C and during a gradual decrease of the ambient temperature to 10°C. Chronic treatment with IL-4 had no effect on body weight (Fig. 5a) or body composition (Fig. 5b,c) as compared to vehicle controls. Measurement of resting metabolic rate revealed no differential effect caused by IL-4 at any tested temperature, and we observed no difference between WT and *Ucp1*$^{-/-}$ mice (Fig. 5d,e). Of note, insulation, defined as the inverse of the slope of the Scholander plot at sub-thermoneutral conditions, also revealed no effect of IL-4 in thermal conductance in either WT or *Ucp1*$^{-/-}$ mice (Fig. 5f). IL-4 treatment induced *Arg1* expression in BAT of cold-exposed mice lacking *Ucp1* relative to control, again confirming successful M2 polarization by IL-4 (Fig. 5g). We further assessed BAT Ucp1 mRNA and protein levels to confirm the genotype of the *Ucp1*$^{-/-}$ and WT mice (Fig. 5h,i). Notably, the protein amount of UCP1 in BAT remained unaffected by IL-4 treatment of WT mice (Fig. 5i). Taken together, these data strongly imply that alternatively activated macrophages do not directly regulate thermogenesis *in vitro* or *in vivo*.

Macrophages do not express *TH* or synthesize catecholamines

To assess the ability of macrophages to synthesize catecholamines, we studied *TH* expression in a reporter mouse expressing tdTomato under control of the TH promoter (TH-cre:r26tdTomato). FACS analysis readily revealed tdTomato-labeled CD11b^{+} CD14^{+} F4/80^{+} cells, that represent macrophages, in Pan-r26-tdTomato control mice, that served as positive control (Fig. 6a). However, we detected no tdTomato signal in BAT macrophages of TH-cre:r26dTomato reporter mice maintained at room temperature nor after exposure of mice to 4°C for 8 h (Fig. 6a). This is consistent with the observation that a peripheral hematopoetic cell-specific *TH* deletion does not affect energy expenditure (Fig. 2c,d). Furthermore, we also

detected no double positive cells in histological analysis following TH staining of BAT sections of Cx3cr1cre:r26-YFP mice (Fig. 6b) or following 2-photon microscopy of CX3CR1GFP :THcre:r26dTomato double reporter animals (Fig. 6c). Finally and corroborating the inability of macrophages to produce TH, RNA sequencing of macrophage populations isolated from various tissues, including BAT, revealed no *TH* transcripts in any of the tested macrophage populations (Fig. 6d). Assessment of *TH* expression in iWAT revealed likewise no mRNA expression of *TH* (Fig. S7). Besides, we detected no co-localization of TH and Mac-2 signal in iWAT or BAT at either room temperature or cold exposure (5°C) (Fig. 8a,b). Of note, in the brown adipose tissue we were only able to detect a very low number of Mac-2-positive macrophages at all (Fig. S8b,c).

We further evaluated a previously proposed role of adiponectin in M2 polarization and thermogenesis in subcutaneous (inguinal) white adipose tissue[9]. We found that protein concentrations of adiponectin are lower, rather than higher, in cold-acclimatized mice (4°C for 4-5 wk) relative to mice maintained at thermoneutrality, while *Adipoq* mRNA levels remained unchanged (Fig. S9). Exposure of WT mice to 4°C for 6 h lead to higher mRNA levels of *Ucp1* and *Pgc-1α* (Fig. S10a,b), but notably lower expression of markers indicative of M1 and M2 polarization (Fig. S10c,d), suggesting that macrophage density reduces during cold-induced sympathetic stimulation of iWAT. HPLC analysis of catecholamines revealed higher absolute levels of dopamine, 3,4-dihydroxyphenylacetic acid, 3-methoxytyramine and homovanillic acid in BAT of cold-exposed mice relative to mice held at room temperature (22°C) (Fig. S10e-h). BAT levels of NE and epinephrine are reduced in the cold-exposed mice relative to room temperature controls, likely reflecting enhanced NE turnover during cold stimulation (Fig. S10i,j).

In summary, these data demonstrate that peripheral, hematopoetic cell-specific *TH* deficiency does not affect energy expenditure, and that macrophages lack the capacity to produce sufficient catecholamines to promote thermogenic effects in iWAT or BAT.

Discussion

Thermogenesis is critical for the survival of homeotherms and plays a key role in energy homeostasis. There is solid evidence indicating that thermogenesis is regulated via the sympathetic nervous system through the release of NE and that consequent activation of β-adrenergic receptors induces lipolysis and drives BAT thermogenesis[10,11]. Given the therapeutic potential of targeting thermogenesis to improve metabolic diseases, it is of high biological and clinical relevance to determine if there are alternative mechanisms that regulate WAT lipolysis and BAT thermogenesis. Hence, it is important to examine if catecholamines are produced by sources other than the SNS and/or the adrenal gland, as that could lead to the identification of targetable pathways for the development of novel therapeutics. Recent studies suggested that M2 macrophages represent one such alternative source of catecholamines. Specifically, it was reported that M2 macrophages synthesize NE *de novo*, and in a paracrine fashion, locally activate β-adrenergic receptor signaling in nearby WAT and BAT adipocytes to induce lipolysis and BAT thermogenesis[6,7]. Furthermore, meteorin-like, a circulating hormone secreted from adipose tissue upon cold exposure, has recently been proposed to potentially promote non-shivering thermogenesis through enhanced recruitment of M2 type macrophages[12]. Similarly, it has been suggested that adiponectin induces browning of subcutaneous WAT by inducing M2 macrophage proliferation upon cold stimulation[9]. Recently, another immune cell type, Type 2 innate lymphoid cells (ILC2s), has been reported to elicit activation of alternative macrophages via IL-4 receptor signaling and to play a role in regulation of beige fat biogenesis[13]. Moreover, caloric restriction has recently been shown to promote browning of white adipose tissue through type 2 cytokine signaling[14], although caloric restriction did not affect

levels of ILC2 in those studies. Of note, it has been shown that IL33-elicited ILC2s promote beiging independently of eosinophils or Il4ra signaling pathway[15].

If alternatively activated macrophages are indeed an important source of catecholamines through de novo synthesis of catecholamines that drive WAT lipolysis, subcutaneous WAT browning and BAT thermogenesis, then one would predict that the elimination of catecholamine production in hematopoetic cells should impair all three processes. To test this hypothesis, we generated a mouse model that allows for the inducible deletion of *TH* in all peripheral tissues, including the bone marrow, and performed a bone marrow transplant into WT mice. Upon acceptance of the BM transplant and replacement of an average of 92% with donor-derived macrophages, we successfully induced *TH* deletion. Notably, the irradiation before the bone marrow transplantation also ablates tissue macrophages[16,17]. In particular, we did not observe any alteration in thermogenesis, energy expenditure or browning of subcutaneous WAT after *TH* knockdown in recipient mice. We also studied the direct effects of alternatively activated macrophages on the thermogenic program of adipocytes *in vitro*, and observed no relevant effect of M2 macrophages on white and brown adipocyte function.

Our studies also investigated a role of alternatively activated macrophages in cold-triggered brown fat function and thermogenesis in multiple *in vivo* and *in vitro* systems. Collectively, these studies indicate that IL-4-mediated polarization to M2 macrophages does not affect energy expenditure or thermogenesis in iWAT/BAT of WT, *Il4ra*$^{-/-}$ and *Ucp1*$^{-/-}$ mice exposed to different ambient temperatures. Further, these studies failed to detect TH expression in CX3CR1-positive mononuclear phagocytes, as revealed by flow cytometry and RNA sequencing analysis, even after cold exposure. Absolute levels of NE, as well as of other intermediates or products of catecholamine synthesis, remained unchanged in IL-4-activated M2 macrophages

co-cultured with primary brown adipocytes and cells/supernatant from IL-4-stimulated BMDMs. Consistent with the lack of TH expression and NE production in macrophages, the inducible deletion of *TH* in bone marrow chimera failed to demonstrate any impairment in energy metabolism, even upon cold exposure. Since previous studies argued for a role of M2 macrophages in thermogenesis and browning of iWAT[6,7,9], the source for the discrepant results remains elusive. For instance, the diverging findings could arise from differences in the composition of the gut microbiome in the mice used here relative to the original reports, or could be due to different animal housing conditions between institutions. Such seemingly insignificant factors have been shown to impact metabolic phenotypes in mouse colonies from different facilities[18]. However, the fact that we used several mouse models, different background strains, and that we performed these studies at several institutions and continents make this scenario unlikely. While previous studies report that *in vitro* macrophages release NE into the culture media[19], it is important to note that the serum used in cell culture contains NE. It is also of interest that osteoblasts, a cell type that is derived from the same lineage as macrophages express the norepinephrine transporter (NET), exhibit specific NE uptake activity via NET and can catabolize, but not generate, NE[20]. Hence, macrophages, just like neurons, may be able to take up and release catecholamines, a process that may be regulated by IL-4 signaling.

In summary, the herein presented studies from six independent laboratories repeatedly and consistently demonstrate that alternatively activated macrophages do not relevantly affect adipocyte metabolism and adaptive thermogenesis by catecholamine production. Instead, we reconfirm the essential and pivotal role of sympathetic activation in regulation of adipose tissue lipolysis and thermogenesis.

Data availability

RNA sequencing data have been deposited in Gene Expression Omnibus and accession codes are available as described[21].

Dedication

We would like to dedicate this manuscript to the memory of Tim Bartness whose work delineates the important role of the SNS in adipose tissue function.

Acknowledgements

We thank A. Fedl, L. Sehrer, L. Müller, S. Jall, D. Heine, T. Stankiewicz for assistance with *in vitro* and *ex vivo* analysis. This work was supported by grants from the German Research Foundation DFG-TS226/1-1 (to T.D.M), DFG-TS226/3-1 (to T.D.M), DFG He3260/8-1 (to S.H.); the EU FP7 Network "DIABAT", the EU ITN Network "TRAIN" 721531 (to S.H.); NIH R01 AA023416, DK082724 and a Career development award from the American Diabetes Association (to C.B); NIH R01DK099222 (to S.D.); the Israeli Science Foundation and European Research Council (AdvERC grant 340345) (to S.J.) and the Swedish Research Council and the Knut and Alice Wallenberg Foundation (to J.N. and B.C.).

Authors Contributions

K.F. co-conceptualized the project, designed and performed *in vitro*, *in vivo* and *ex vivo* experiments, analyzed and interpreted data and wrote the manuscript. B.F. and C.C. helped design experiments and interpreted data. H.H.R., K.J., V.vdH, A.C.S., D.H. performed, analyzed and interpreted the inducible THΔper mouse, validation of antibodies and BM chimera data. A.V.K. and N.P. performed, analyzed and interpreted *in vivo* experiments in *Ucp1*$^{-/-}$ mice. J.N. and K-W.S. performed, analyzed

and interpreted catecholamine data. Y.W. and S.J. performed, analyzed and interpreted tyrosine hydroxylase staining. F.B. generated the *Il4ra*$^{-/-}$ mouse. S.D., E.G., S.K., M.J., D.M., G.C., S.H., J.N., B.C. helped design experiments and interpreted data. S.C.W. helped with interpretation of data and drafting the manuscript. M.H.T. co-conceptualized the project and interpreted all data. T.D.M and C.B. co-conceptualized the project, interpreted all data, supervised the studies and wrote the manuscript.

Competing financial interests

The authors declare no competing financial interests.

References

1 Jastroch, M. *et al.* Seasonal Control of Mammalian Energy Balance: Recent advances in the understanding of daily torpor and hibernation. *Journal of neuroendocrinology*, doi:10.1111/jne.12437 (2016).

2 Cannon, B. & Nedergaard, J. Brown adipose tissue: function and physiological significance. *Physiological reviews* **84**, 277-359, doi:10.1152/physrev.00015.2003 (2004).

3 Oelkrug, R., Polymeropoulos, E. T. & Jastroch, M. Brown adipose tissue: physiological function and evolutionary significance. *Journal of comparative physiology. B, Biochemical, systemic, and environmental physiology* **185**, 587-606, doi:10.1007/s00360-015-0907-7 (2015).

4 Cypess, A. M. & Kahn, C. R. Brown fat as a therapy for obesity and diabetes. *Current opinion in endocrinology, diabetes, and obesity* **17**, 143-149, doi:10.1097/MED.0b013e328337a81f (2010).

5 Bartelt, A. *et al.* Brown adipose tissue activity controls triglyceride clearance. *Nature medicine* **17**, 200-205, doi:10.1038/nm.2297 (2011).

6 Nguyen, K. D. *et al.* Alternatively activated macrophages produce catecholamines to sustain adaptive thermogenesis. *Nature* **480**, 104-108, doi:10.1038/nature10653 (2011).

7 Qiu, Y. *et al.* Eosinophils and type 2 cytokine signaling in macrophages orchestrate development of functional beige fat. *Cell* **157**, 1292-1308, doi:10.1016/j.cell.2014.03.066 (2014).

8 Thomas, S. A., Matsumoto, A. M. & Palmiter, R. D. Noradrenaline is essential for mouse fetal development. *Nature* **374**, 643-646, doi:10.1038/374643a0 (1995).

9 Hui, X. *et al.* Adiponectin Enhances Cold-Induced Browning of Subcutaneous Adipose Tissue via Promoting M2 Macrophage Proliferation. *Cell metabolism* **22**, 279-290, doi:10.1016/j.cmet.2015.06.004 (2015).

10 Hsieh, A. C. & Carlson, L. D. Role of adrenaline and noradrenaline in chemical regulation of heat production. *The American journal of physiology* **190**, 243-246 (1957).

11 Bartness, T. J., Vaughan, C. H. & Song, C. K. Sympathetic and sensory innervation of brown adipose tissue. *International journal of obesity* **34 Suppl 1**, S36-42, doi:10.1038/ijo.2010.182 (2010).

12 Rao, R. R. *et al.* Meteorin-like is a hormone that regulates immune-adipose interactions to increase beige fat thermogenesis. *Cell* **157**, 1279-1291, doi:10.1016/j.cell.2014.03.065 (2014).

13 Lee, M. W. *et al.* Activated type 2 innate lymphoid cells regulate beige fat biogenesis. *Cell* **160**, 74-87, doi:10.1016/j.cell.2014.12.011 (2015).

14 Fabbiano, S. *et al.* Caloric Restriction Leads to Browning of White Adipose Tissue through Type 2 Immune Signaling. *Cell metabolism* **24**, 434-446, doi:10.1016/j.cmet.2016.07.023 (2016).

15 Brestoff, J. R. *et al.* Group 2 innate lymphoid cells promote beiging of white adipose tissue and limit obesity. *Nature* **519**, 242-246, doi:10.1038/nature14115 (2015).

16 Merad, M. *et al.* Langerhans cells renew in the skin throughout life under steady-state conditions. *Nature immunology* **3**, 1135-1141, doi:10.1038/ni852 (2002).

17 Ginhoux, F. *et al.* Fate mapping analysis reveals that adult microglia derive from primitive macrophages. *Science* **330**, 841-845, doi:10.1126/science.1194637 (2010).

18 Ussar, S., Fujisaka, S. & Kahn, C. R. Interactions between host genetics and gut microbiome in diabetes and metabolic syndrome. *Molecular metabolism* **5**, 795-803, doi:10.1016/j.molmet.2016.07.004 (2016).

19 Flierl, M. A. *et al.* Phagocyte-derived catecholamines enhance acute inflammatory injury. *Nature* **449**, 721-725, doi:10.1038/nature06185 (2007).

20 Ma, Y. *et al.* Extracellular norepinephrine clearance by the norepinephrine transporter is required for skeletal homeostasis. *J Biol Chem* **288**, 30105-30113, doi:10.1074/jbc.M113.481309 (2013).

21 Lavin, Y. *et al.* Tissue-resident macrophage enhancer landscapes are shaped by the local microenvironment. *Cell* **159**, 1312-1326, doi:10.1016/j.cell.2014.11.018 (2014).

Figure Legends

Figure 1. Selective deletion of *TH* in peripheral but not CNS tissues results in peripheral catecholamine depletion and impaired thermoregulation.

Schematic of the inducible peripheral *TH* knockout (THΔper) mouse model (**a**). TH protein expression in the brain and peripheral tissues after induction (**b**). Representative TH Western blot images of samples from WT or THΔper in brain stem, BAT, spleen, liver, eWAT. Uncropped Western blot images are shown in Supplementary Figure 11 and comprise for WT and THΔper mice *n* = 4 and *n* = 6 samples (brain stem), *n* = 7 and *n* = 5 (BAT), *n* = 4 and *n* = 6 (spleen), *n* = 4 and *n* = 4 (liver) and *n* = 1 and *n* = 3 (eWAT). Gapdh of eWAT was chosen as a representative image for the loading control; comparable Gapdh loading for other tissues is shown in Supplementary Figure 11. Level of norepinephrine in peripheral tissues of WT (*n* = 3-5) and THΔper (*n* = 3-4) mice, each dot representing one animal. (**c**). Body temperature of WT (*n* = 7) and THΔper mice (*n* = 7) during a cold tolerance test at 4°C (**d**). Data represent mean ± s.e.m. Asterisks indicate: *, p<0.05; **, p<0.01; *** p<0.001 based on 2-sided student's ttest (**c**) or 2-way analysis of variance (ANOVA) followed by Bonferroni post-hoc comparison of the individual time-points (**d**).

Figure 2. Energy expenditure of WT and THΔper chimera.

Percent donor-derived hematopoietic cells in peripheral blood 8 wks after bone marrow transplantation from WT (*n* = 5) or THΔper mice into WT mice (*n* = 5), designated from here on as WT chimera and THΔper chimera (FSC: forward scatter, SSC sided scatter) (**a**). Body weight of chimera (**b**). Oxygen consumption (**c**,**d**), total locomotor activity (**e**) and RER (**f**) during a successive reduction in ambient temperatures (21, 15, 10, or 6°C). Rectal temperature of WT (*n* = 4) and THΔper chimera (*n* = 4), exposed to either 10 or 6°C for 24 h (**g**). Gene expression of browning and brown fat thermogenesis markers (*Dio2*, *Tnf*, *Prdm16*, *Pgc-1α, Ucp1*) in iWAT from WT (*n* = 4) and THΔper chimera (*n* = 4) after 24-h exposure to or 6°C (h). Data represent means ± s.e.m. Asterisks indicate: *, p<0.05; **, p<0.01. Data were analyzed using 2-sided student's ttest (**a**,**b**,**d**,**e**,**g**,**h**), analysis of co-variance (ANCOVA) with body weight as covariate (**c**), or 2-way ANOVA followed by Bonferroni post-hoc comparison (**f**).

Figure 3. Effect of alternatively activated macrophages from BALB/c mice on thermogenesis in primary inguinal white and brown adipocytes.

Representative expression profile of M2 macrophage markers (*Arg1, Mrc1, Mgl2*) in IL-4-treated BMDM cells (**a**-**c**) (graph shows 1 out of 3 independently performed experiments). Gene expression of brown fat-specific markers (*Ucp1, Pgc-1α*) in IL-4 conditioned media (CM) or isoproterenol (Iso)-treated iWAT (**d**,**e**) or BAT (**f**,**g**) primary cells for 6 h. Displayed results are representative for three independently performed experiments, each performed with *n* = 3 technical replicates. Representative Western blot (**h**) and quantification (**i**) of phosphorylated or total HSL of 6-d differentiated BAT primary cells treated with CM from IL-4 treated BMDMs or Iso (1 μM) for 6 h. Western blot in panel **h** shows one out of three independently performed experiments, each performed with *n* = 3 technical replicates. Uncropped Western blot images are shown in Supplementary Figure 11. Data represent means ± s.e.m. Asterisks indicate: *, p<0.05; **, p<0.01; ***, p<0.001 based on 1-way ANOVA followed by Bonferroni-multiple comparison test.

Figure 4. Effect of IL-4 on energy expenditure and thermogenesis in WT and *Il4ra*$^{-/-}$ mice at different temperatures.

Body weight (**a**) and energy expenditure of saline (Vhcl) or IL-4 (50 μg/kg)-treated WT (*n* = 8 and *n* = 7) (**b**) or *Il4ra*$^{-/-}$ mice (*n* = 7 each treatment) (**c**) was recorded over 4 d with ambient temperature decreasing from 30°C to 20°C to 10°C to 5°C (24-h measurement for each temperature). Gene expression of M2 macrophage markers *Arg1* (**d**), *Mrc1* (**e**), *Mgl2* (**f**), brown fat-specific markers *Ucp1* (**g**), *Pgc-1α* (**h**), and Interleukin-4 receptor alpha, *Il4ra* (**i**) of BAT from cold-exposed WT or *Il4ra*$^{-/-}$ mice treated with either vehicle (*n* = 7-8 and *n* = 6-7) or IL-4 (*n* = 6-7 each treatment), each dot representing one animal. Protein analysis (**j**-**n**), of iWAT and BAT from cold-exposed WT mice treated with either vehicle (*n* = 6) or IL-4 (*n* = 6). Uncropped Western blot images are shown in Supplementary Figure 11. Catecholamines and metabolites (norepinephrine, 3,4-dihydroxyphenylacetic acid (DOPAC), 3-methoxytyramine (3-MT), homovanillic acid (HVA) and dopamine) were measured in BAT from cold-exposed mice treated with vehicle (*n* = 7) or IL-4 (*n* = 7) (**o**). Data represent means ± s.e.m. Asterisks indicate: *, p<0.05; **, p<0.01; ***, p<0.001. Data were analyzed using 1-way ANOVA followed by Bonferroni-multiple comparison test

(**a**,**d**-**i**), analysis of co-variance (ANCOVA) with body weight and body composition (fat and lean tissue mass) as covariate (**b**,**c**) or 2-sided student's ttest (**k**,**m**-**o**).

Figure 5. Effect of IL-4 on thermogenesis in WT and *Ucp1*$^{-/-}$ mice.
Body weight (**a**) and body composition (**b**,**c**) of saline (Vhcl) or IL-4 (50 µg/kg)-treated WT and *Ucp1*$^{-/-}$ mice. Scholander plot of vhcl (*n* = 11) or IL-4 (*n* = 11) treated WT (**d**) or *Ucp1*$^{-/-}$ (*n* = 8 each treatment) (**e**) mice and calculated insulation of all groups (**f**). Gene expression of *Arg1* (**g**) and *Ucp1* (**h**) (*n* = 4-5 WT and *n* = 3-4 *Ucp1*$^{-/-}$ each treatment; each dot representing one animal), as well as protein levels of Ucp1 (**i**) from BAT of WT and *Ucp1*$^{-/-}$ mice treated with vhcl (*n* = 4 WT and *n* = 4 *Ucp1*$^{-/-}$) or IL-4 (*n* = 5 WT and *n* = 4 *Ucp1*$^{-/-}$). Uncropped Western blot images are shown in Supplementary Figure 12. Data represent means ± s.e.m. Asterisks indicate: *, p<0.05; **, p<0.01; ***, p<0.001 based on 1-way ANOVA followed by Bonferroni-multiple comparison test.

Figure 6. Tyrosine hydroxylase staining of brown adipose tissue macrophages.
Representative FACS analysis of BAT macrophages isolated from pan-tdTomato, WT and *TH*^{Cre}:tdTomato$^{fl/fl}$ mice (*n* = 2 each genotype), either from mice housed at 22°C or at 4°C for 8 h; (top) macrophage gating strategy on CD11b, F4/80 and CD14 expressing cells (**a**). Representative histology of BAT taken from Cx3cr1^{cre}:r26- YFP animals in 22°C, stained for TH (red) and YFP (green) (*n* = 2) (scale bar: 50 µm) (**b**). Representative 2-photon live imaging of BAT taken from *TH*^{Cre}:tdTomato $^{fl/fl}$:Cx3cr1^{gfp} mice at 22°C (*n* = 5) (scale bar: 50 µm) (**c**). Integrative Genomics Viewer (IGV) plots of RNA sequencing data of the *TH* locus of macrophages isolated from brain, BAT, spleen, liver, peritoneum, large and small intestine (Li, SI) under steady state; data are from[21], except for BAT macrophages (**d**). Displayed results in panel **d** were performed in technical duplicates.

Online Methods

General experimental approaches for *in vivo* experiments

For *in vivo* studies, group sizes of 7-8 mice were preferentially used, which was determined from previous experiments where we determined this to be optimal for *in vivo* evaluation. Smaller group sizes were used in the studies utilizing genetically or chemically modified animals in case there were not sufficient numbers available to reach the preferred group size of 7-8.

For measurement of IL-4 induction of energy expenditure, group size estimations were based upon a power calculation to minimally yield an 80% chance to detect a 20% difference in energy expenditure between the treatment groups and under the assumption of an alpha level of 0.05 and a standard deviation of 13% in both groups.

For the *in vivo* studies, mice were randomized into the treatment groups based upon body weight and body composition (fat and lean tissue mass). For *in vivo* experiments, all mice reveal a C57Bl/6 background and experiments were performed non-blinded.

Mice

All animal procedures were approved by either the Mount Sinai School of Medicine, Institutional Animal Care and Use Committee (IACUC) protocols, CCHMC IACUC, the Weizmann Institute Animal Care Committee, the Animal Ethics Committee of the North Stockholm region or the regional animal welfare committee of the state of Bavaria.

We generated inducible peripheral *TH* knockout mice by crossing $TH^{flox/flox}$ mice (kindly provided by Dr Richard Palmiter, University of Washington) with tamoxifen-inducible Rosa26CreERT2 mice (Taconic #6466, Hudson, NY). The resultant $TH^{flox/flox}$,$Rosa26^{CreERT2+/-}$ mice (THΔper mice) and the $TH^{flox/flox}$,$Rosa26^{CreERT2-/-}$ (WT littermates) expressed normal levels of TH protein during development and before tamoxifen induction of the KO. Deletion of the TH gene was achieved by tamoxifen administration and was limited to the periphery due to low expression of cre

recombinase in the CNS[22]. Here, we used male 28 wk old WT or THΔper mice (*n* = 4 each genotype).

To generate mice with inducible *TH* deficiency (THΔper chimera) restricted to hematopoetic cells, we injected 4 x 10^6 T-cell-depleted BM cells from non-induced THΔper (CD45.2$^+$) (*n* = 2 males and *n* = 3 females, age of 14 wk) or WT (CD45.1$^+$) (*n* = 2 males and *n* = 3 females, age of 4-8 wk) mice i.v. into lethally irradiated (2x600 rads) CD45.1$^+$ congenic (B6.SJL-Ptprc^a Pepc^b/BoyJ; #002014; The Jackson laboratories, USA) (*n* = 2 males and *n* = 3 females, age of 4-8 wk) or WT (CD45.2$^+$) (*n* = 2 males and *n* = 3 females, age of 19-22 wk at injection) mice as described[23]. We assessed reconstitution of the immune system ~8 wk later by differentiating donor- (CD45.2$^+$) and host-derived cell populations in peripheral blood according to CD45.1/CD45.2 expression patterns and used mice with a donor reconstitution of >90% for all subsequent experiments.

We used the following mouse strains to generate reporter mice: *cx3cr1$^{gfp/+}$* mice (JAX stock 005582 B6.129P-Cx3cr1tm1Litt/J, *cx3cr1^{Cre} (*JAX stock 025524 B6J.B6N(Cg)-Cx3cr1tm1.1(cre)Jung/J); *tdTomato* reporter mice (JAX stock 007908 B6.129S6-Gt(ROSA)26Sor<tm14(CAG-tdTomato)Hze>/J) and *TH^{Cre}* mice (male 8 wk old mice). All animals were on C57Bl/6 background and maintained under specific pathogen-free (SPF) conditions.

Analysis of mouse metabolic phenotypes

We analyzed body composition (fat and lean mass) using a magnetic resonance whole-body composition analyzer (EchoMRI, Houston, TX). We assessed of energy intake, energy expenditure and home-cage activity by usage of an indirect calorimetric system (TSE PhenoMaster, TSE Systems, Bad Homburg, Germany). Data for energy expenditure were analyzed using analysis of covariance (ANCOVA) with body weight and body composition (fat and lean tissue mass) as covariates as previously described[24].

IL-4 pharmacology studies

To assess the effect of IL-4 on energy expenditure, we treated male C57Bl/6J and *Il4ra$^{-/-}$* mice (4 mo of age) daily for 12 consecutive days via intraperitoneal

administration of either vehicle (0.9% saline, Braun, Melsungen, Germany) or recombinant IL-4 (50 µg/kg; Peprotech, Rocky Hill, NJ). Mice were acclimatized to the metabolic chambers for 24 h prior to start of the measurement. Prior to study Day 9, mice were kept at thermoneutrality (30°C) and then housed for 24 h at 20°C followed by 24 h at 10°C and 24 h at 5°C. We then sacrificed mice for subsequent tissue analysis and catecholamine quantification.

We backcrossed mice lacking Ucp1 (*Ucp1*$^{-/-}$) (progeny of those described in[25]) to C57Bl/6 for more than 10 generations, and after intercrossing, mice lacking Ucp1 (*Ucp1*$^{-/-}$) were maintained in parallel with the WT C57Bl/6 mice. They were fed ad libitum (R70 Standard Diet, Lactamin), had free access to water, and were kept at a 12:12h light/dark cycle, at the normal (22°C) vivarium temperature. To determine the effect of IL-4 on energy expenditure, male WT and *Ucp1*$^{-/-}$ mice were acclimatized to 30°C at least 4 wk prior to experiment. We treated 4 mo old mice daily (at 11:00 h) for 8 consecutive d via intraperitoneal administration of either vehicle (0.9% saline) or recombinant IL-4 (50 µg/kg; Peprotech, Rocky Hill, NJ) at 30°C. On Day 9, mice were placed into indirect calorimetry metabolic chambers (INCA, Somedic, Horby, Schweden) with free access to food and water. After overnight acclimatization at 30°C, the temperature in the chambers was gradually decreased to 10°C (2-3 h at each temperature). After the experiment mice were kept at 30°C for 3 wk for recovery from the treatment. After recovery, mice were inversely assigned to control and treated group (former control mice became treated and *vice versa*) and the experiment was repeated. Mice were finally sacrificed after energy expenditure was recorded. Time between last injection of IL-4 and sacrifice of mice was 48 h. At every ambient temperature, resting metabolic rate was calculated as minimal stable (during at least 10 min) oxygen consumption and was plotted *vs* the ambient temperature ("Scholander plots")[26]. Using total energy expenditure calculated during the last h at each temperature by means of a modified Weir equation yielded similar results[27]. The slopes of the Scholander plots at and below 26-27°C were calculated individually for every mouse using the best linear fit. Insulation was calculated as the inverse of the slope. Two rounds of the experiment yielded similar results.

Western blot

For the THΔper and chimera studies, we homogenized the tissues in 20 mM MOPS containing 2 mM EGTA, 5 mM EDTA, 30 mM sodium fluoride, 40 mM β-glycerophosphate, 10 mM sodium pyrophosphate, 2 mM sodium orthovanadate, 0.5% NP-40 and complete protease inhibitor cocktail (Roche, Nutley, NJ) and centrifuged at 13,000g for 20 min at -4°C. The supernatant was then collected and protein concentration was measured using a bicinchoninic acid (BCA) protein quantification kit (Thermo Scientific, Waltham, MA). Protein extracts were separated on 4-12% NuPAGE gels (Invitrogen, Carlsbad, CA) and blotted onto Immobilon FL PVDF membranes (Millipore, Billerica, MA). Membranes were blocked at room temperature for 1 h with Odyssey LI-COR Blocking Buffer (LI-COR, Lincoln, NE) diluted 1:1 in Tris-buffered saline (TBS). Membranes were then incubated with primary antibodies (diluted 1:1000 in a 1:1 Blocking Buffer/TBS-T solution) overnight at 4°C. Primary antibodies against tyrosine hydroxylase (EMD Millipore, Billerica MA-MAB318) and Gapdh (Santa Cruz Biotechnology, Dallas, TX -32233) were used. Membranes were washed consecutively 3 times for 5 min each in TBS-T (0.1%). Blots were incubated with Dylight 680-conjugated goat anti–rabbit IgG and Dylight 800-conjugated goat anti–mouse IgG (Thermo Scientific, Waltham, MA) for 1 h at room temperature in blocking buffer containing 0.1% TBS-T and 0.1% SDS. Blots were washed 3 more times in TBS-T followed by a final wash in TBS, and the blots were then scanned with the LI-COR Odyssey (LI-COR, Lincoln, NE) and quantified with Odyssey 3.0 software based on direct fluorescence measurement. Other fat tissues were lysed in ice-cold RIPA buffer (Sigma Aldrich, Munich, Germany) containing 1 mM PMSF (Carl Roth), 10 nM Calyculin A (Cell signaling) and protease/phosphatase inhibitor (Thermo Fisher Scientific, Erlangen, Germany) using a polytron. Lysates were chilled on ice for 20 min and centrifuged for 15 min, 10,000 g, at 4°C. The supernatant was collected and protein concentration was as described above. Proteins were separated on a Criterion gel (Bio-Rad, Munich, Germany) and transferred on to nitrocellulose membranes. Membranes were incubated with primary antibody (Cell Signaling Technology, Danvers, MA) overnight at 4°C, and HRP-coupled secondary antibody (Santa Cruz Biotechnology, Dallas, TX) was utilized to detect protein signal via the LI-COR imaging system. Antibodies were purchased from Cell signaling (Phospho-HSL (Ser660) #4126, HSL #4107), Santa Cruz (Gapdh G-9, #365062) and Abcam (Ucp1, #23841).

Flow cytometry

We performed FACS analysis of BM chimera using CD45.1 and CD45.2 antibodies (Biolegend). Acquisition was performed with a BDBioscienes FACSCalibur and analysis with FlowJo software. For the FACS analysis of BAT of the *TH*^{cre}:dTomato$^{f/f}$:CX3CR1^{gfp} mice, tissue was collected, dissected by scissors and then incubated for 30 min with DMEM medium (Beit Ha'emek, Israel) containing 1 mg/ml collagenase-2 (Sigma-Aldrich), 2% BSA (Sigma-Aldrich) and 12.5 mM HEPES buffer (Beit-Ha'emek, Israel). The resulting cell suspension was filtered through a 70 µm mesh and erythrocytes were removed by ACK lysis. Following cell suspension, cells were incubated in FACS buffer (PBS with 1% BSA, 2 mM EDTA and 0.05% sodium azide) in the presence of staining antibody. Antibodies used for staining were CD45 (clone 30F11, Biolegend), CD14 (clone Sa2-8, Biolegend) and F4/80 (clone BM8, Serotech).

Preparation of RNA and gene expression analysis

Total RNA was prepared using RNeasy Kit (Qiagen, Hilden, Germany) according to manufacturer's instructions. cDNA synthesis was performed with QuantiTect Reverse Transcription Kit (Qiagen, Hilden, Germany) according to manufacturer's instructions. Gene expression of cell samples (n = 3 per group) was profiled with quantitative PCR-based (qPCR-based) techniques using SYBR green or TaqMan Single Probes (Thermo Fisher Scientific, Erlangen, Germany). The relative expression of the selected genes was measured using the 7900HT Fast Real-Time PCR System (Thermo Fisher Scientific, Erlangen, Germany). The relative expression levels of each gene were normalized to the housekeeping gene peptidylprolyl isomerase B (*Ppib*), hypoxanthine phosphoribosyltransferase (*Hprt*) or TATA box binding protein (*Tbp*). RNA expression data were quantified according to the ΔC_t method as described[28]. Sequences of all primers are listed in supplementary table 1. TaqMan Low Density Array (Thermo Fisher Scientific, Erlangen, Germany) was performed according to instructions.

Isolation and culture of BMDMs

Bone marrow from the hind legs of 6-wk-old C57Bl/6 or BALB/c mice was harvested, erythrocytes were lysed with ACK buffer (151 mM NH_4Cl, 10 mM $KHCO_3$, 0.2 mM EDTA in H_2O) and the bone marrow was purified using Ficoll (GE Healthcare,

Munich, Germany). Monocyte differentiation into macrophages was achieved by differentiation with DMEM medium containing 30% L929 supernatant, 20% FBS and 1% Pen/Strep for 5 d. BMDMs polarization towards the M2 phenotype was accomplished by treatment with IL-4 (5, 10, 20 ng/ml, Peprotech, Rocky Hill, NJ) for 24 h.

Isolation of primary adipocytes

Inguinal white adipose tissue was obtained from 6-8-wk-old male C57Bl/6J or BALB/c mice. Fat pads were minced and digested for 40 min at 37°C (1 mg/ml Collagenase IV (Thermo Fisher Scientific, Erlangen, Germany); 3 U/ml Dispase II (Sigma Aldrich, Munich, Germany); 0.01 mM $CaCl_2$ in PBS). The cell suspension was filtered, centrifuged and resuspended in growth medium (DMEM/F12 1:1 plus Glutamax (Thermo Fisher Scientific, Erlangen, Germany) containing 1% Pen/Strep and 10% FBS. Primary white adipocytes were grown to confluence (37°C, 10% CO_2) followed by induction of differentiation using dexamethasone (1 µM), isobutylmethylxanthine (0.5 mM), rosiglitazone (1 µM) and insulin (5 µg/ml) in growth medium. After 48 h induction, cells were maintained in culture medium containing insulin (5 µg/ml) and rosiglitazone (1 µM). On Day 4 of differentiation, cells were cultured in growth medium containing insulin (5 µg/ml). To stimulate thermogenesis, cells were treated with 0.5-1 µM isoproterenol (Sigma Aldrich, Munich, Germany) dissolved in serum-free growth medium, for 6 h on Day 6 of adipocyte differentiation.

Primary brown adipocytes were isolated via the same procedure with the exception that 1 mg/ml Collagenase II (Thermo Fisher Scientific, Erlangen, Germany) was used for digestion. For differentiation of primary brown adipocytes, the induction cocktail contained dexamethasone (5 µM), isobutylmethylxanthine (0.5 mM), rosiglitazone (1 µM), indomethacine (125 µM), T3 (1 nM) and insulin (0.5 µg/ml) in growth medium. At 2-d post-induction of differentiation, cells were maintained in culture medium containing rosiglitazone (1 µM), T3 (1 nM) and insulin (0.5 µg/ml). On Day 4 of differentiation, cells were cultured in growth medium containing T3 (1 nM) and insulin (0.5 µg/ml). For β-adrenergic receptor activation, primary brown adipocytes were treated with 1 µM isoproterenol (Sigma Aldrich, Munich, Germany), dissolved in serum-free growth medium, for 6 h on Day 6 of adipocyte differentiation.

Catecholamine measurement

For sample preparation: 100 µl $HClO_4$ (0.3 M) and 4 µl of internal standard (DHBA, 1 ng/µl) were added to the cell pellets. The mixture was ultra-sonicated under ice for 10 sec and transferred into an Amicon Ultra 0.5 ml (3 kDa) centrifugal filter unit (Merck Millipore, Darmstadt, Germany). The samples were then centrifuged at 13,000 rpm for 30 min at 1°C. The filtrate was transferred into a measurement vial and injected into the system. The supernatant was thawed and 200 µl were transferred into an Amicon Ultra 0.5 ml (3 kDa) centrifugal filter unit (Merck Millipore, Darmstadt, Germany). 4 µl of internal standard (DHBA, 1 ng/µl) were added and the samples were centrifuged at 13,000 rpm for 30 min at 1°C. The filtrate was transferred into a measurement vial and injected into the system. The BAT was thawed and 200 µl of perchloric acid (0.3 M) and 4 µl of internal standard (DHBA, 1 ng/µl) were added. The samples were homogenized by ultrasonication for 30 sec on ice. For this, they had to be in a 1.5 mL Eppendorf tube, as bigger tubes with their level lower end are not sufficient for the homogenization. Afterwards, the samples were centrifuged at 9,000 rpm for 10 min at 1°C. The residue was usually at the bottom of the tube, so that the supernatant could be directly transferred into a measurement vial and injected into the system. If the fat layer was on top, the solution had to be taken with a 1 ml syringe fitted with a cannula and filtered through a 0.2 µm syringe filter (Whatman, Maidstone, United Kindom) into the sample vial and was then injected into system. Measurement of monoamines and metabolites: 20 µl were injected into an Ultimate 3000 HPLC system from Thermo Fischer, consisting of an isocratic pump, an autosampler, and a coulometric Ultra Analytical Cell (6011 RS). The potential was set to 0.4 mV with a data collection rate of 25 Hz. The separation of the compounds was carried out on a C_{18}-column from Waters (Atlantis T3 100Å, 3 µm, 4.6 mm X 150 mm), with a preceding security guard cartridge (Phenomenex, AJ0-4287). An isocratic elution with a commercially available mobile phase from RECIPE (1210, ClinRep® commercial HPLC) with 5.5% (v/v) added acetonitrile and a flow rate of 0.5 ml/min was used.

Histology and 2-photon imaging

For immunofluorescence, tissues fixed in 4% paraformaldehyde (PFA) overnight at 4°C, incubated with 30% sucrose for 48 h and flash-frozen with isopentane before sectioning by cryostat. Samples were blocked with PBS containing 0.05% Tween

(PBS-T), 0.3% triton and 20% normal horse serum (NHS) before incubation with PBS-T containing 0.3% triton, 2% NHS and primary antibodies in 4°C, followed by incubation with secondary antibody in PBS at RT for 1 h and final stain with Hoechst (1:25,000). Antibodies used were anti-GFP/YFP (Abcam) and anti-TH (Millipore). For 2-photon imaging, interscapular BAT was isolated from indicated animals and subjected to two-photon microscopy using an upright LSM 880 NLO combined confocal-multi-photon system, (Zeiss, Germany) with Chameleon Ultra tunable Ti:Sapphire laser, Coherent (USA) with Plan-Apochromat 20x/0.8 M27 lens. For excitation of tdTomato and GFP the laser was tuned to 900 nm and the emission filter set was 578 – 638 nm and 519 – 561 respectively. Image acquisition and further visualization was performed using ZEN Imaging software (Zeiss, Germany).

RNA Isolation of BAT macrophages, Library Construction, and Analysis

RNA-seq was performed as described previously[21]. In brief, 10^4 cells were sorted into 50 µl of lysis/binding buffer (Life Technologies) and stored at -80°C. mRNA was captured with Dynabeads oligo (dT) (Life Technologies) according to manufacturer's guidelines. We used a derivation of MARS-seq[29] to produce expression libraries with a minimum of two replicates per population. Four million reads per library were sequenced and aligned to the mouse reference genome (NCBI 37, mm9) using HISAT v0.15 with default parameters. Expression levels were calculated and normalized for each sample to the total number of reads using HOMER software (http://homer.salk.edu)[30]. RNA-seq analysis focused on genes in 25th percentile of expression with a 2-fold differential between at least two populations. The value of k for the K-means clustering (matlab function kmeans) was chosen by assessing the average silhouette (matlab function evalclusters; higher score means more cohesive clusters) for a range of possible values with correlation as the distance metric.

Depletion of macrophages from primary iWAT

Macrophages were separated from iWAT primary cells by magnetic immunoaffinity isolation using anti-CD11b antibodies conjugated to magnetic beads (MACS Cell Separation System; Miltenyi Biotec, Bergisch Gladbach, Germany). Following iWAT isolation, CD11b-positive cells were separated using positive selection columns (LD columns; Miltenyi Biotec, Bergisch Gladbach, Germany) according to manufacturer's

instructions. For validation of cell separation, cell eluents were taken before and after depletion of CD11b-positive cells as well as from the retained cell fraction, bound to the conjugated beads. Successful depletion of macrophages was confirmed by flow cytometric and qPCR analysis.

Oil Red O staining and Microscopy

Cells were fixed with 4% PFA at differentiation Day 0, 3 or 6. Adipocytes were stained with Oil Red O (Sigma Aldrich, Munich, Germany) for 10 min and immediately washed with H_2O. Phase contrast microscopy was performed before and after Oil Red O staining with a Keyence BZ-9000 microscope. For lipid quantification, Oil Red O was retrieved from the cells by 100% isopropanol and absorbance was measured at 500 nm. Dapi signal was measured to correct for cell number.

Bioenergetic analysis

Primary iWAT cells were isolated, macrophage-depleted and differentiated for 5 d on a collagen-coated XF96 well plate. On the day of the experiment (Day 5), cells were washed with DMEM XF Assay medium (Seahorse Bioscience, Santa Clara, CA), supplemented with 25 mM glucose, 10 mM pyruvate and 0.3% fatty-acid free BSA, and incubated in 180 µl of XF Assay medium in a non-CO2 incubator at 37°C for 1 h. All port compounds were dissolved in pure DMEM XF Assay medium without supplements and 10-fold higher concentrated compounds were loaded into the ports of a XF Assay Cartridge. Oxygen consumption rate (OCR) was measured using an extracellular flux analyzer (XF96, Seahorse Bioscience, Santa Clara, CA). Basal OCR was recorded for 21 min followed by measurement of OCR after injection of isoproterenol (1 µM, 35 min), oligomycin (2 µg/ml, 21 min), carbonyl cyanide-p-trifluoromethoxyphenylhydrazone (FCCP) (1 µM, 21 min), rotenone (2.5 µM)/antimycin (2.5 µM)/2-Deoxyglucose (10 mM) (28 min). For normalization, the cell plate was subsequently co-stained with Dapi and Nile red and the fluorescence signal was detected to correct for cell number and differentiation.

Adipocyte treatment with conditioned media from activated macrophages

Conditioned media from 24-h polarized BMDMs or Raw264.7 cells (Sigma Aldrich, Munich, Germany) were collected and supplemented to 6-d differentiated primary adipocytes for 6 h. Raw264.7 cells have been tested for mycoplasma contamination.

Immunofluorescence

Inguinal white and interscapular brown adipose tissues were dissected from room temperature (23°C) or 4-h cold-exposed (5°C) C57Bl/6J mice and subsequently fixed in 4% PFA. Fat tissues was embedded in paraffin and cut in 5 µm sections in a vibratome. After deparaffinization, sections were subjected to antigen retrieval by boiling for 20 min in citrate buffer (10 mM Sodium citrate in H_2O, pH = 6) in a microwave, then left to cool at room temperature for 20 min. After washing in TBS, sections were blocked in SUMI (0,25% gelatine + 0,5% TritonX in TBS) for 1 h, then incubated overnight at 4°C with a cocktail containing primary antibodies against TH (ab152, abcam, 1:500) and Mac-2 (CL8942AP, CedarLane Labs, 1:500) diluted in SUMI. After washing in TBS, sections were incubated with a cocktail of secondary antibodies (Alexa 488 Goat anti-rabbit, R37116 + Alexa 568 Goat anti-rat, A-11077) diluted in SUMI for 1 h at room temperature. After washing in TBS, sections were incubated with 0,1% Sudan Black B (Sigma Aldrich, Munich, Germany) in 70% EtOH for 20 min to quench autofluorescence then washed with TBS + 0,02% Tween20. Sections were then counter-stained for 3 min with Dapi (Thermo Fisher Scientific, 62248, 1:3000), washed in TBS, then mounted using Elvanol mounting medium. Image stacks (5 µm thick) were collected through the z-axis at an interval of 1 µm using a Leica SP5 scanning confocal microscope equipped with a 20x and 40x objective, and final images obtained by maximum intensity projection of the z-stack. Number of Mac-2-positive cells was quantified using ImageJ, for each sample (n = 3-4), the average number of cells was calculated from at least three different 20x fields from at least two different sections.

Statistics

Statistical analyses were performed using statistical tools implemented in GraphPad Prism (version 6). Statistical analyses were performed on data distributed in a normal pattern using a regular one-way or two-way analysis of variance (ANOVA) with Bonferroni *post hoc* multiple comparison analysis to determine statistical significance between treatment groups. Differences with P values less than 0.05 were considered

significant. Group size estimations were based upon a power calculation to minimally yield an 80% chance to detect a significant difference in energy expenditure or body weight of $P < 0.05$ between the treatment groups. All results are given as mean ± s.e.m. Data on gene expression were screened for singular statistically significant outliers using the maximum normed residual (Grubb's) test implemented in GraphPad prism.

Methods-only References

21 Lavin, Y. *et al.* Tissue-resident macrophage enhancer landscapes are shaped by the local microenvironment. *Cell* **159**, 1312-1326, doi:10.1016/j.cell.2014.11.018 (2014).

22 Koch, L. *et al.* Central insulin action regulates peripheral glucose and fat metabolism in mice. *J Clin Invest* **118**, 2132-2147, doi:10.1172/JCI31073 (2008).

23 Homann, D. *et al.* Lack of intrinsic CTLA-4 expression has minimal effect on regulation of antiviral T-cell immunity. *Journal of virology* **80**, 270-280, doi:10.1128/JVI.80.1.270-280.2006 (2006).

24 Tschop, M. H. *et al.* A guide to analysis of mouse energy metabolism. *Nature methods* **9**, 57-63, doi:10.1038/nmeth.1806 (2011).

25 Enerback, S. *et al.* Mice lacking mitochondrial uncoupling protein are cold-sensitive but not obese. *Nature* **387**, 90-94, doi:10.1038/387090a0 (1997).

26 Scholander, P. F., Walters, V., Hock, R. & Irving, L. Body insulation of some arctic and tropical mammals and birds. *The Biological bulletin* **99**, 225-236, doi:10.2307/1538740 (1950).

27 Weir, J. B. New methods for calculating metabolic rate with special reference to protein metabolism. *The Journal of physiology* **109**, 1-9 (1949).

28 Livak, K. J. & Schmittgen, T. D. Analysis of relative gene expression data using real-time quantitative PCR and the 2(-Delta Delta C(T)) Method. *Methods* **25**, 402-408, doi:10.1006/meth.2001.1262 (2001).

29 Jaitin, D. A. *et al.* Massively parallel single-cell RNA-seq for marker-free decomposition of tissues into cell types. *Science* **343**, 776-779, doi:10.1126/science.1247651 (2014).

30 Heinz, S. *et al.* Simple combinations of lineage-determining transcription factors prime cis-regulatory elements required for macrophage and B cell identities. *Mol Cell* **38**, 576-589, doi:10.1016/j.molcel.2010.05.004 (2010).

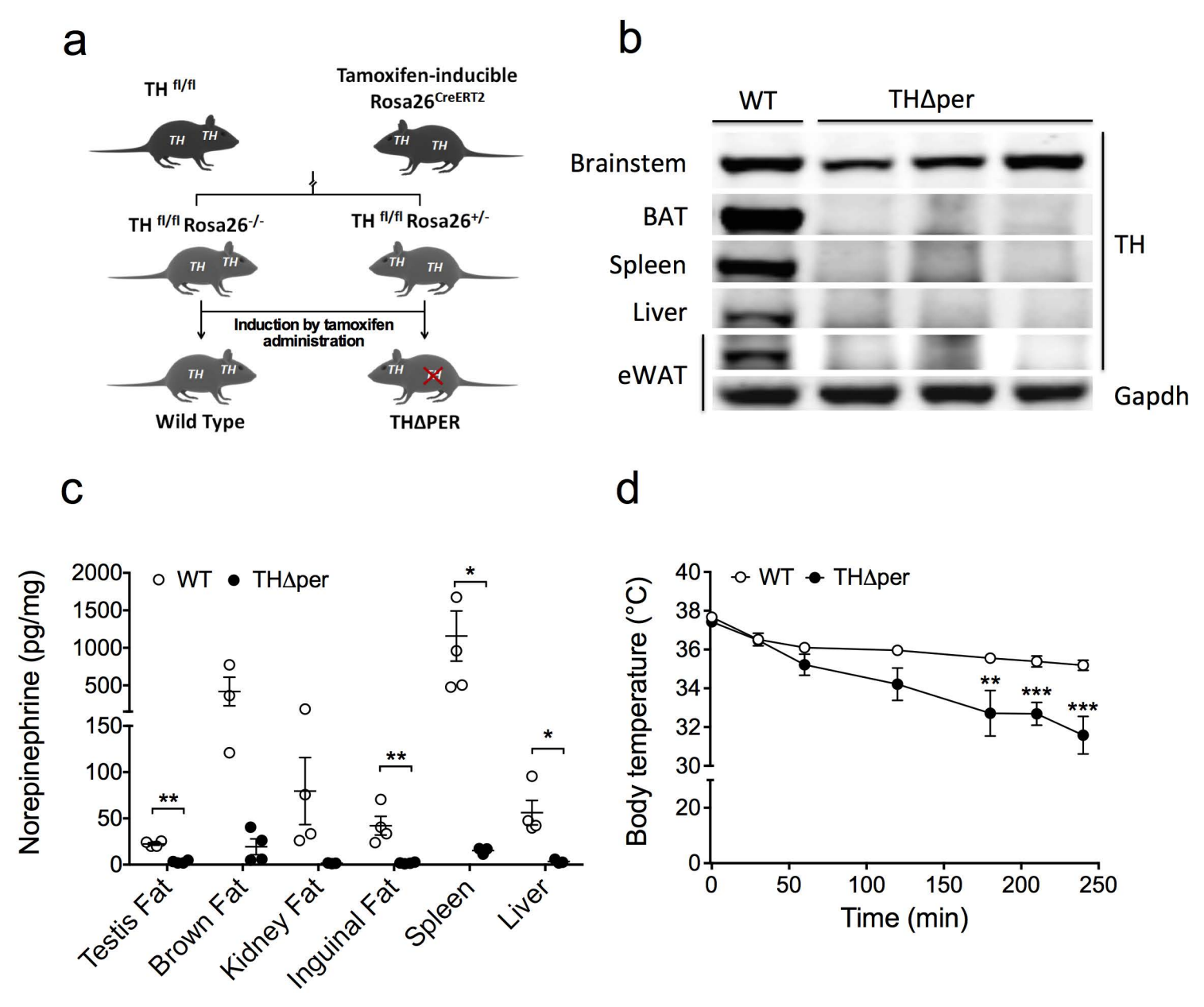
a
TH fl/fl
Tamoxifen-inducible
Rosa26CreERT2
TH fl/fl Rosa26-/-
TH fl/fl Rosa26+/-
Induction by tamoxifen administration
Wild Type
THΔPER
b
WT
THΔper
Brainstem
BAT
Spleen
Liver
eWAT
TH
Gapdh
c
Norepinephrine (pg/mg)
WT
THΔper
Testis Fat
Brown Fat
Kidney Fat
Inguinal Fat
Spleen
Liver
d
Body temperature (°C)
Time (min)

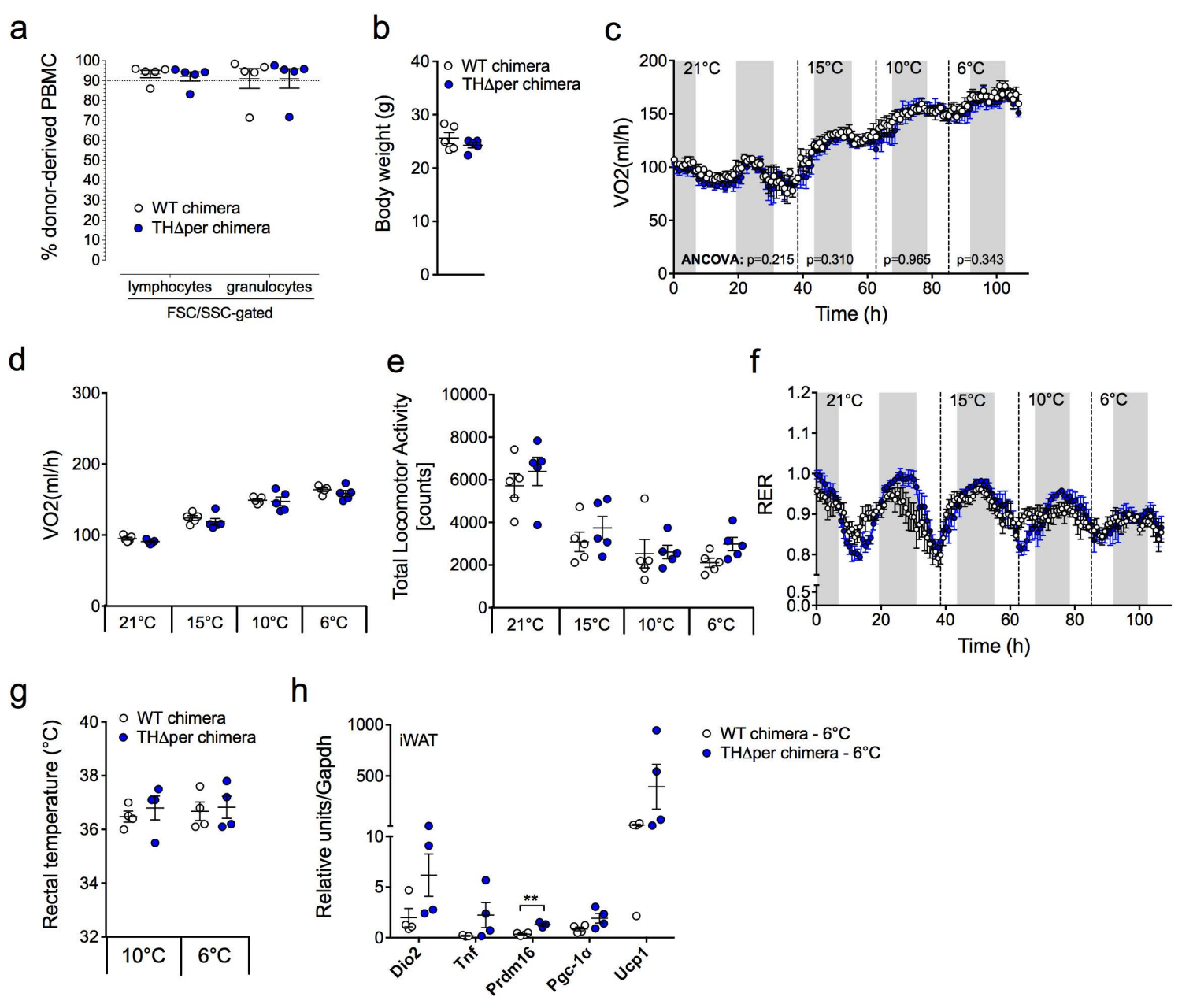
a
% donor-derived PBMC
WT chimera
THΔper chimera
lymphocytes
granulocytes
FSC/SSC-gated
b
Body weight (g)
WT chimera
THΔper chimera
c
VO2(ml/h)
21°C
15°C
10°C
6°C
ANCOVA: p=0.215
p=0.310
p=0.965
p=0.343
Time (h)
d
VO2(ml/h)
21°C
15°C
10°C
6°C
e
Total Locomotor Activity [counts]
21°C
15°C
10°C
6°C
f
RER
21°C
15°C
10°C
6°C
Time (h)
g
Rectal temperature (°C)
WT chimera
THΔper chimera
10°C
6°C
h
Relative units/Gapdh
iWAT
WT chimera - 6°C
THΔper chimera - 6°C
**
Dio2
Tnf
Prdm16
Pgc-1α
Ucp1

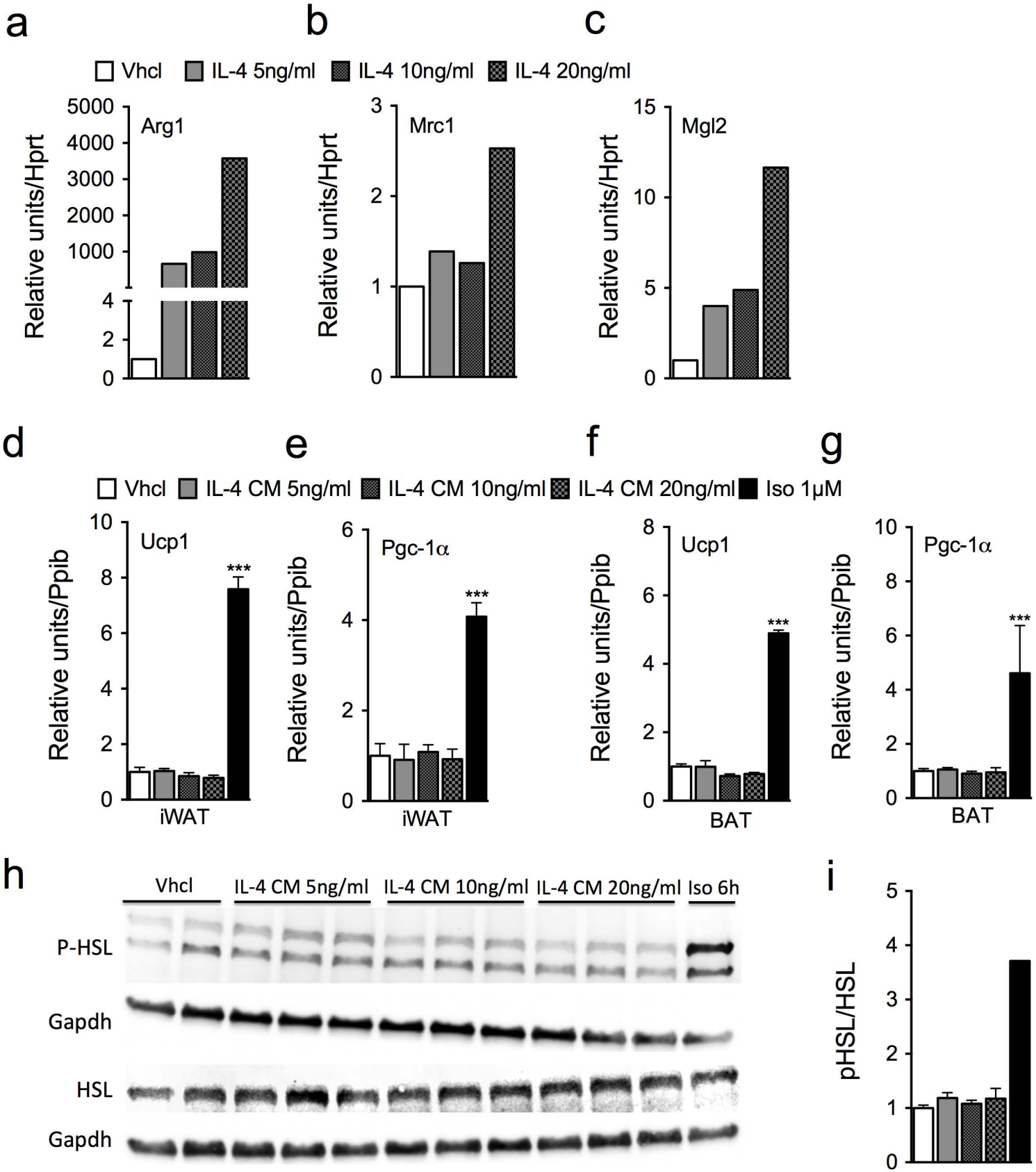
a
b
c
Vhcl
IL-4 5ng/ml
IL-4 10ng/ml
IL-4 20ng/ml
Arg1
Mrc1
Mgl2
Relative units/Hprt
d
e
f
g
Vhcl
IL-4 CM 5ng/ml
IL-4 CM 10ng/ml
IL-4 CM 20ng/ml
Iso 1μM
Ucp1
Pgc-1α
Relative units/Ppib
***
iWAT
BAT
h
Vhcl
IL-4 CM 5ng/ml
IL-4 CM 10ng/ml
IL-4 CM 20ng/ml
Iso 6h
P-HSL
Gapdh
HSL
Gapdh
i
pHSL/HSL

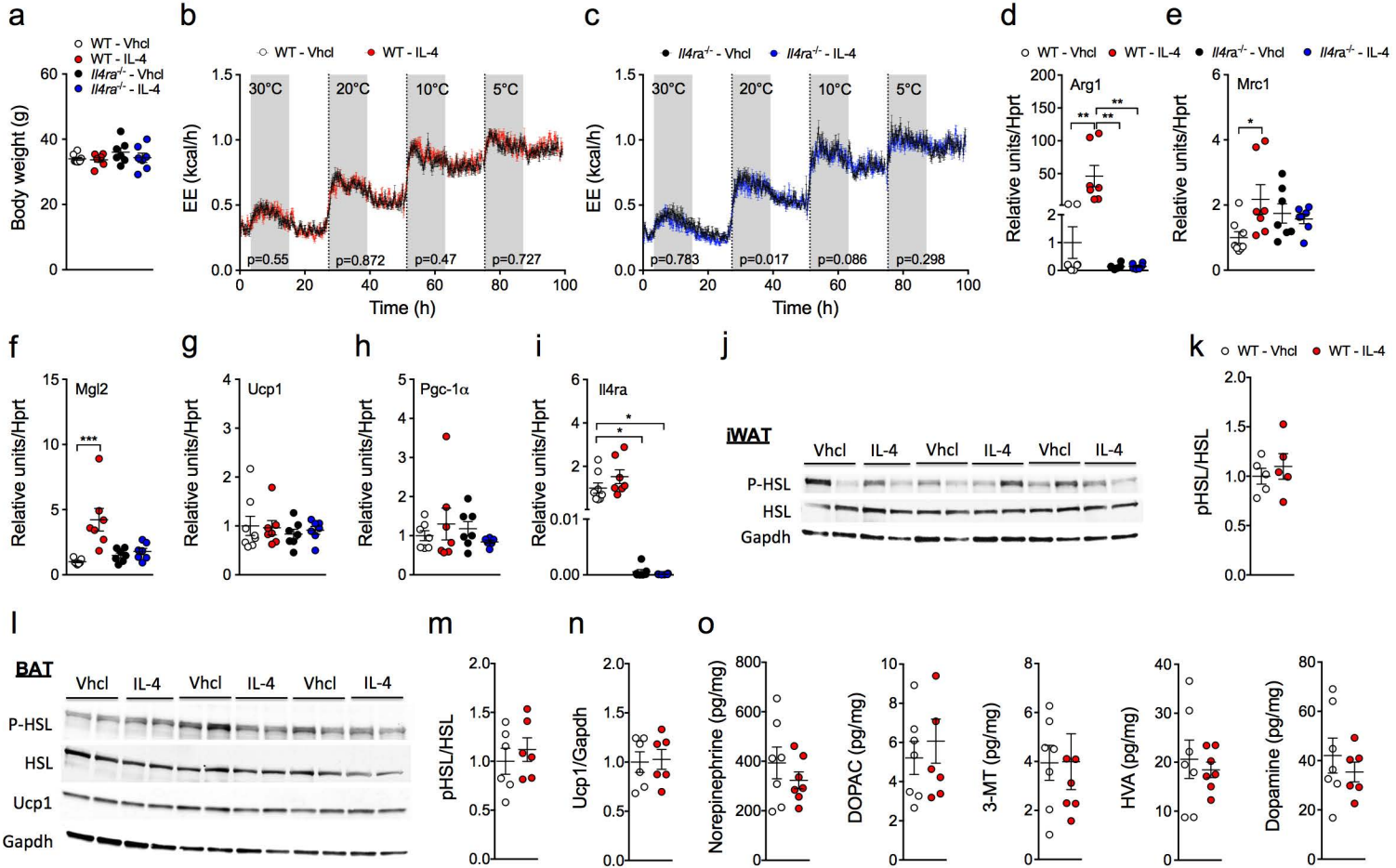
a
WT - Vhcl
WT - IL-4
Il4ra-/- - Vhcl
Il4ra-/- - IL-4
Body weight (g)
b
WT - Vhcl
WT - IL-4
30°C
20°C
10°C
5°C
EE (kcal/h)
p=0.55
p=0.872
p=0.47
p=0.727
Time (h)
c
Il4ra-/- - Vhcl
Il4ra-/- - IL-4
p=0.783
p=0.017
p=0.086
p=0.298
Time (h)
d
Arg1
Relative units/Hprt
e
Mrc1
Relative units/Hprt
f
Mgl2
Relative units/Hprt
g
Ucp1
Relative units/Hprt
h
Pgc-1α
Relative units/Hprt
i
Il4ra
Relative units/Hprt
j
iWAT
Vhcl
IL-4
P-HSL
HSL
Gapdh
k
pHSL/HSL
l
BAT
Ucp1
m
pHSL/HSL
n
Ucp1/Gapdh
o
Norepinephrine (pg/mg)
DOPAC (pg/mg)
3-MT (pg/mg)
HVA (pg/mg)
Dopamine (pg/mg)

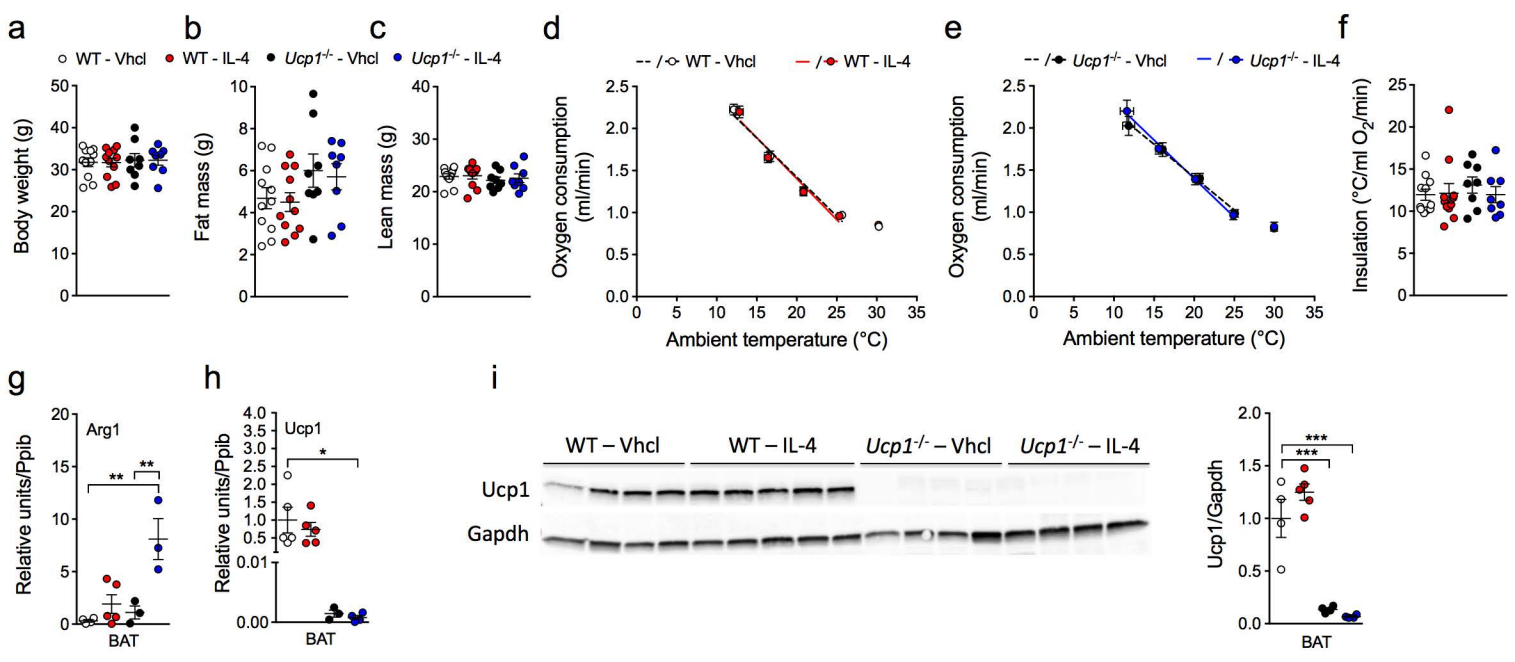
a
b
c
d
e
f
WT - Vhcl
WT - IL-4
Ucp1-/- - Vhcl
Ucp1-/- - IL-4
Body weight (g)
Fat mass (g)
Lean mass (g)
Oxygen consumption (ml/min)
Ambient temperature (°C)
Insulation (°C/ml O2/min)
g
h
i
Arg1
Ucp1
Relative units/Ppib
BAT
WT – Vhcl
WT – IL-4
Ucp1-/- – Vhcl
Ucp1-/- – IL-4
Gapdh
Ucp1/Gapdh

a

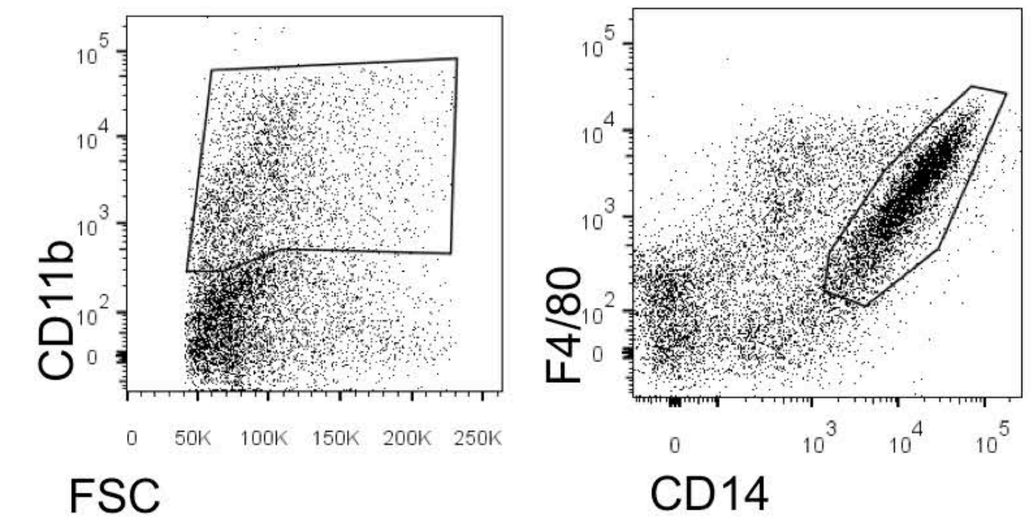
CD11b
FSC
F4/80
CD14

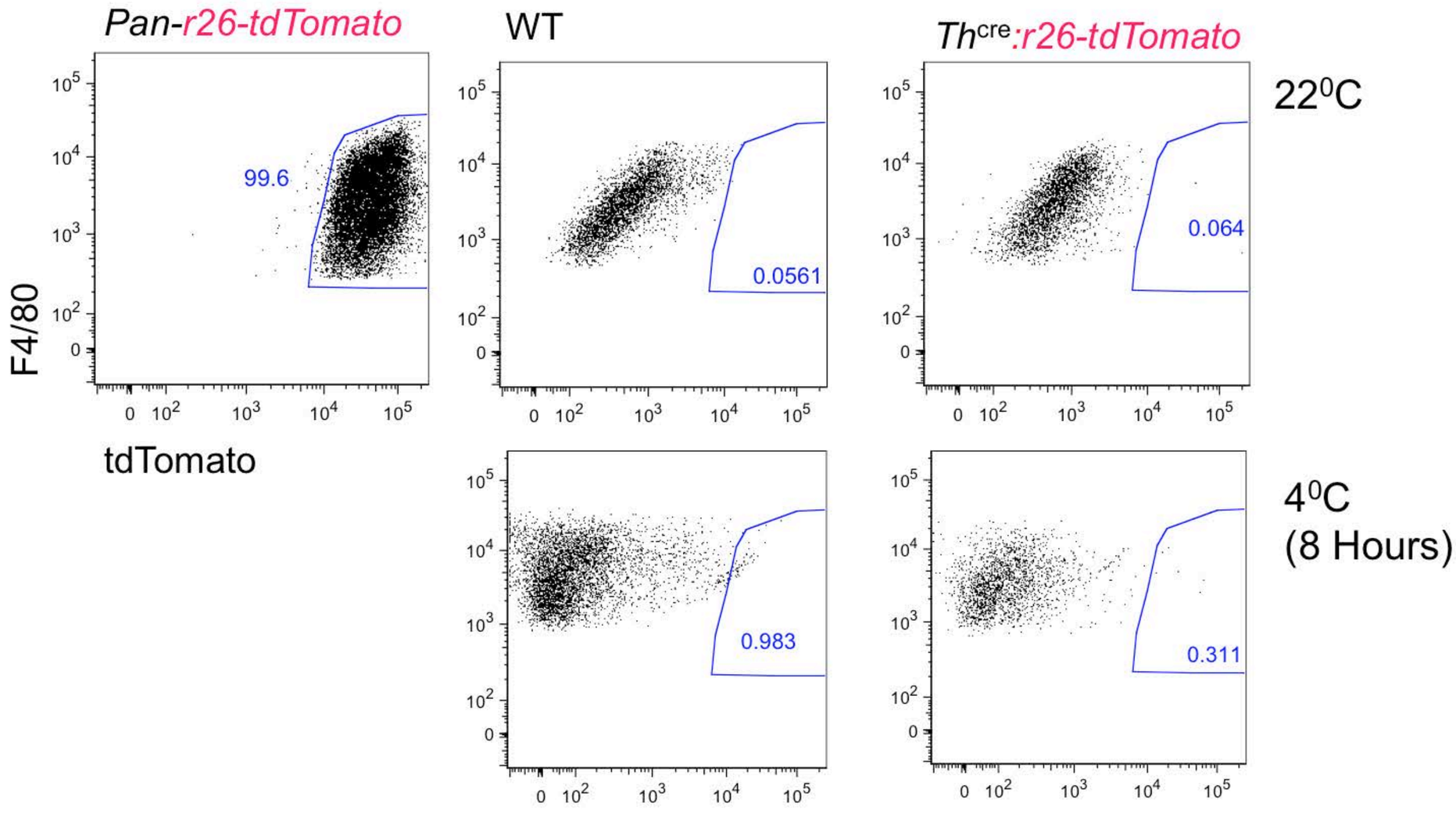
Pan-r26-tdTomato
WT
Thcre:r26-tdTomato
22⁰C
4⁰C
(8 Hours)
F4/80
tdTomato
99.6
0.0561
0.064
0.983
0.311

b

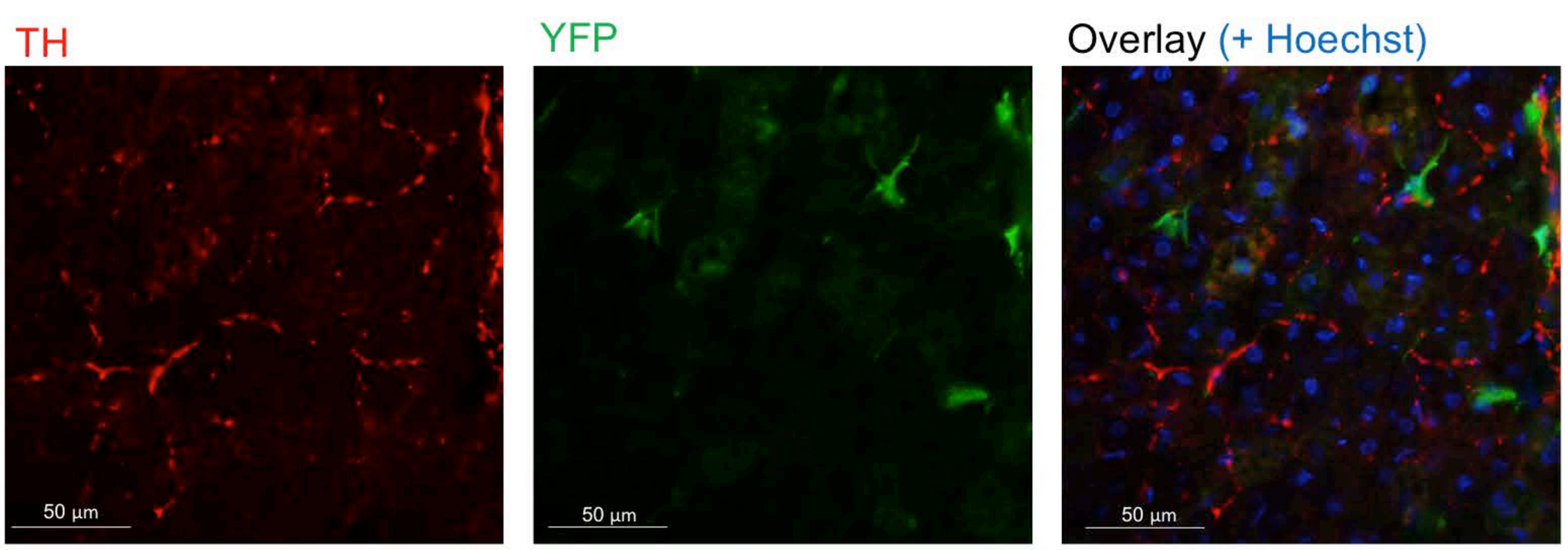
TH
YFP
Overlay (+ Hoechst)
50 µm
50 µm
50 µm

c

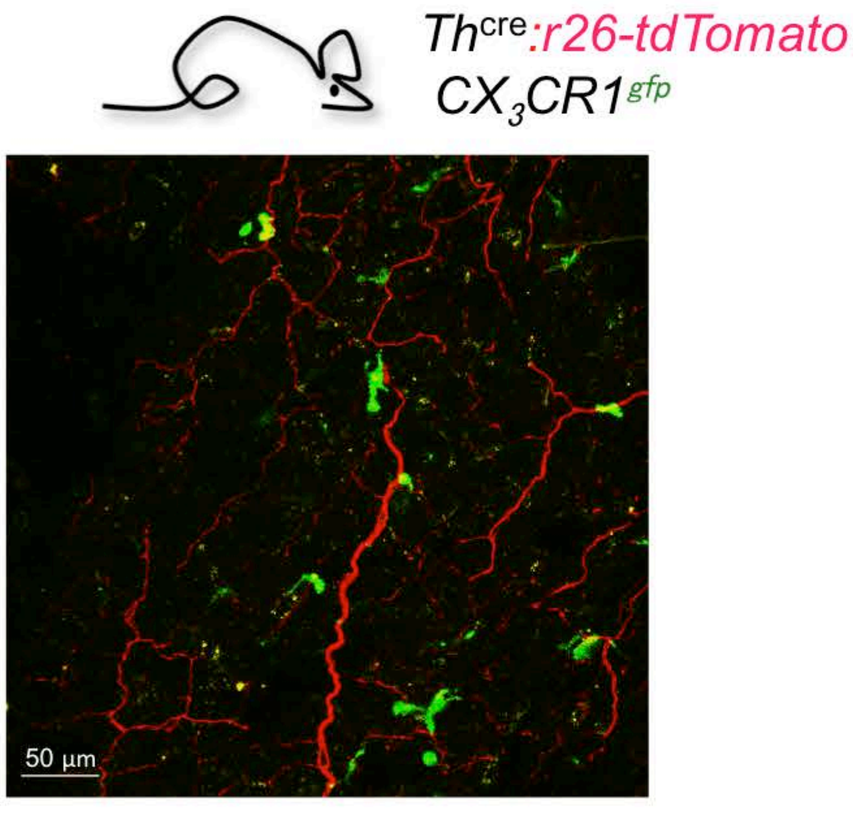
Thcre:r26-tdTomato
CX3CR1gfp
50 µm

d

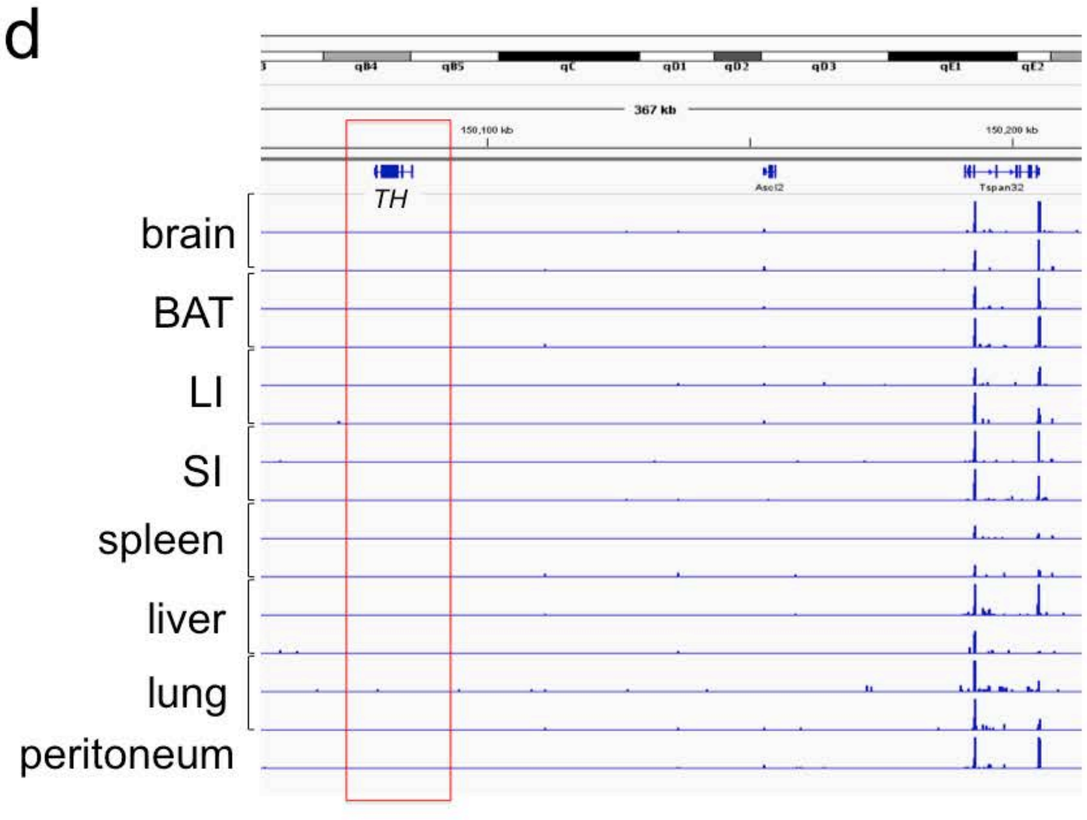
TH
Ascl2
Tspan32
brain
BAT
LI
SI
spleen
liver
lung
peritoneum

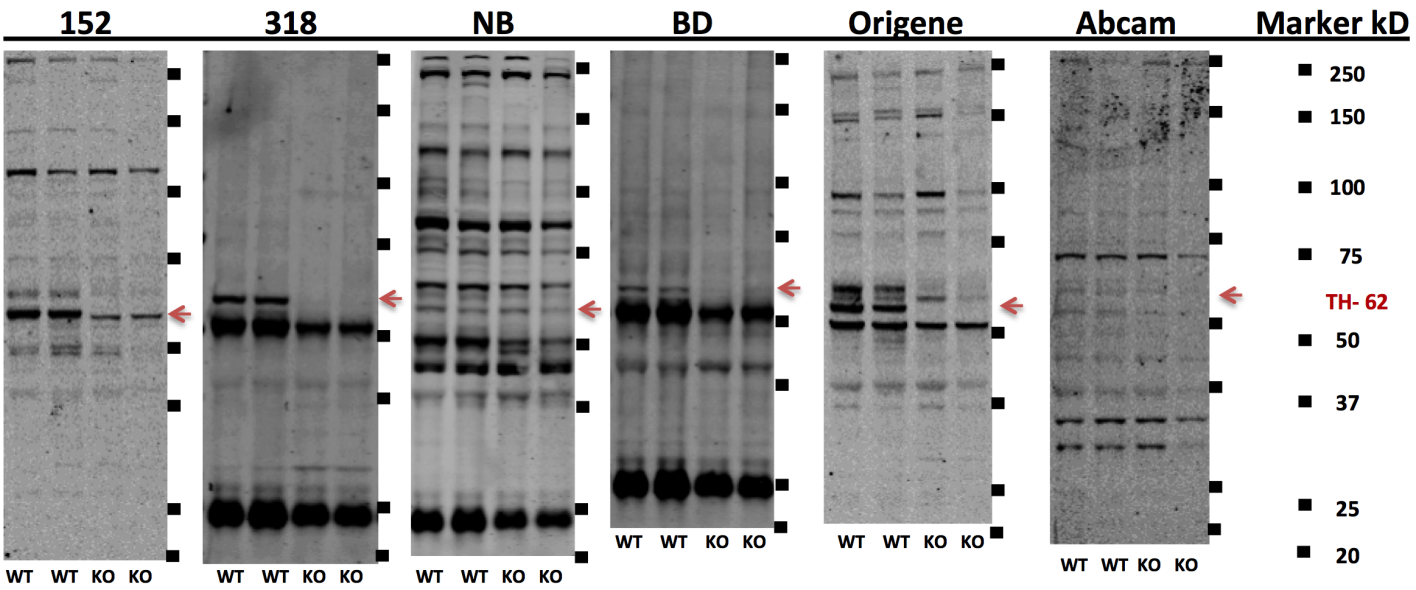

Supplementary Figure 1. Specificity of antibody recognition of TH.
Western blot analysis of the same spleen extracts from WT (*n* = 2) and THΔper mice (KO) (*n* = 2) to evaluate the specificity of the following TH antibodies: 152 (Millipore, Cat#AB152; Lot#2593900); 318 (Millipore, Cat#MAB318; Lot#2523803); NB (Novus Biological, Cat#NBP242212; Lot#A-1); BD (BD Biosciences, Cat#612300; Lot#43397863); Origene (Cat#TA303716; Lot#GR212964); Abcam (Cat#ab41528; Lot#GR226873-1).

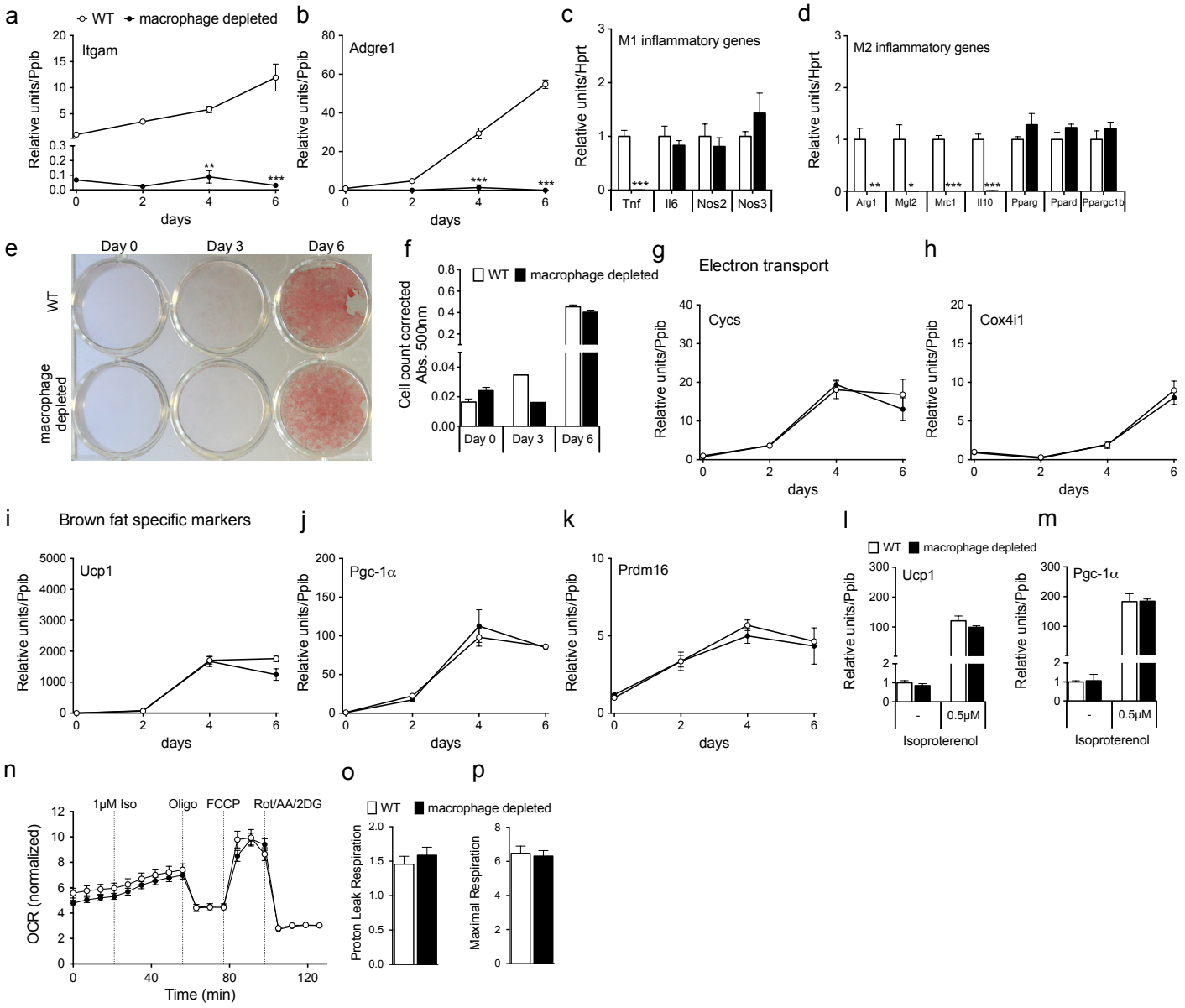

Supplementary Figure 2. Effect of macrophage depletion on lipid accumulation, adipocyte differentiation and browning in primary inguinal white adipocytes.

Expression of macrophage infiltration marker (*Itgam,* alias *CD11b*) (**a**) and (*Adgre1*) (**b**), genes related to M1 inflammation (*Tnf*, *Il6*, *Nos2*, *Nos3*) (**c**) and M2 inflammation (*Arg1*, *Mgl2*, *Mrc1*, *Il10*, *Pparg*, *Ppard*, *Ppargc1b*) (**d**) in WT or macrophage-depleted iWAT primary cells (*n* = 3 each group). Lipid accumulation measured by Oil Red O staining at different time points during adipocyte differentiation (**e**) (image is representative for three independent experiments). Quantification of cell number corrected (Dapi staining) lipid accumulation (Oil Red O incorporation) after re-elution in isopropanol (*n* = 2 technical replicates) (**f**). mRNA levels of electron transport markers (*Cycs, Cox4i1*) (**g**,**h**) and brown fat-specific markers (*Ucp1*, *Pgc1α*, *Prdm16*) (**i**-**k**) in iWAT primary cells during adipocyte differentiation. Expression levels of *Ucp1*, *Pgc1α* following stimulation with isoproterenol (0.5 μM) for 6 h in fully differentiated iWAT primary cells (**l**,**m**). Measurement of oxygen consumption rate (OCR), corrected for cell number (Dapi) of inguinal white adipocytes following treatment with isoproterenol (Iso) (1 μM), oligomycin (2 μg/ml), FCCP (1 μM) and rotenone (2.5 μM)/antimycin A (2.5 μM)/2-Deoxyglucose (10 mM) (**n**). Proton Leak Respiration is calculated as the difference between ATP synthesis during blocked respiration (oligomycin) and non-mitochondrial respiration (**o**). Maximal Respiration is calculated as the difference between FCCP-induced respiration and non-mitochondrial respiration (**p**). Data represent means ± s.e.m. Data shown in S2 **a**-**d**,**g**-**m** are representative for three independently performed experiments, each performed in triplicates. Displayed results in panel **n**-**p** are representative for two independent experiments (*n* = 23 technical replicates per group). Asterisks indicate: *, p<0.05; **, p<0.01; ***, p<0.001 based on 2-way ANOVA followed by Bonferroni post-hoc comparison of the individual time-points (**a**,**b**) or students ttest (**c**,**d**).

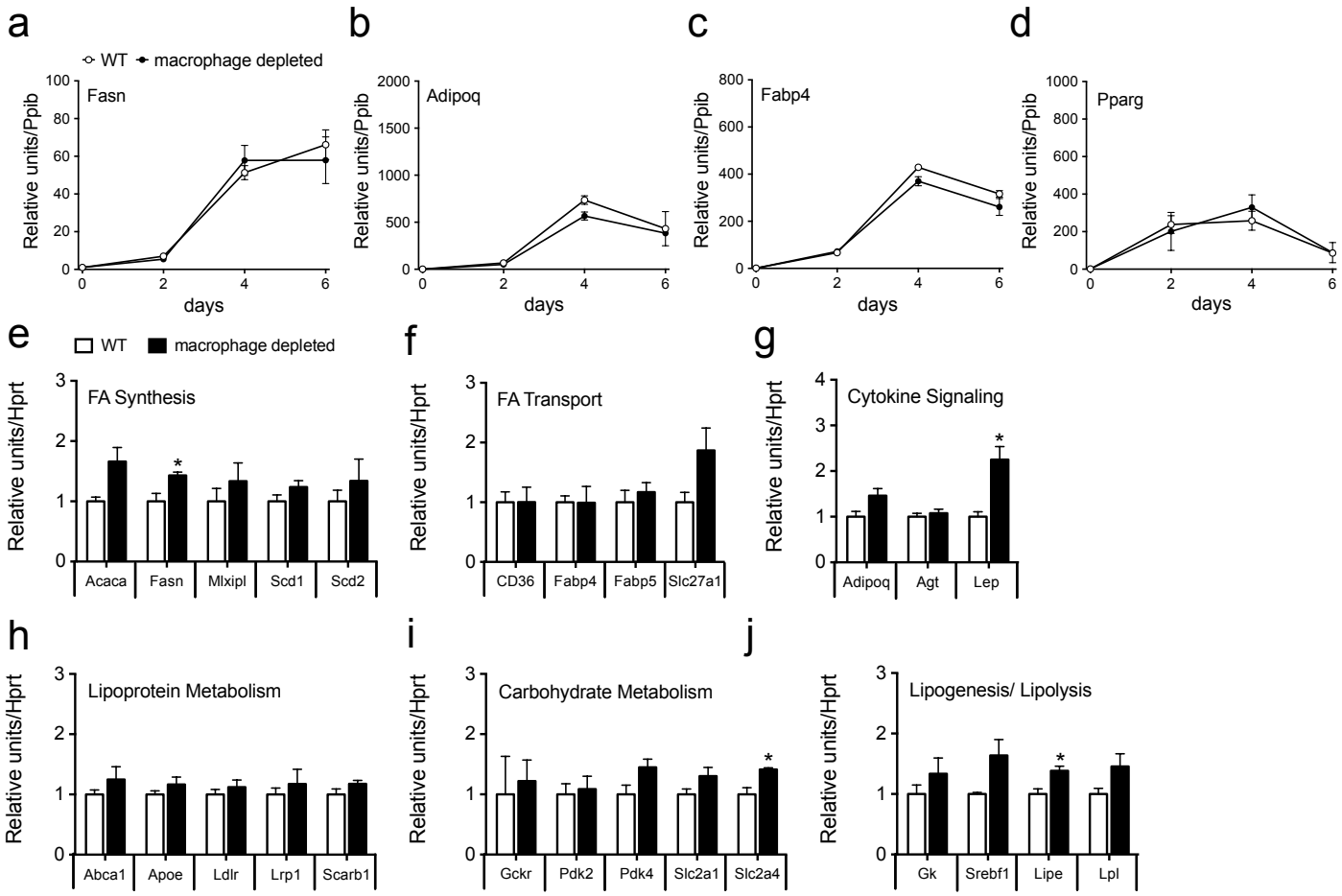

Supplementary Figure 3. Effect of macrophage depletion on key metabolic pathways in primary inguinal white adipocytes.

Expression profile of markers indicative of white adipocyte differentiation (*Fasn*, *Adipoq*, *Fabp4*, *Pparg*) in WT or macrophage-depleted iWAT primary cells (**a**-**d**). Low Density Array analysis of WT and macrophage-depleted iWAT primary cells revealed expression profile of genes related to fatty acid (FA) synthesis (*Acaca*, *Fasn*, *Mlxipl*, *Scd1*, *Scd2*) (**e**), fatty acid transport (*CD36*, *Fabp4*, *Fabp5*, *Slc27a1*) (**f**), cytokine signaling (*Adipoq*, *Agt*, *Lep*) (**g**), lipoprotein metabolism (*Abca1*, *Apoe*, *Ldlr*, *Lrp1*, *Scarb1*) (**h**), carbohydrate metabolism (*Gckr*, *Pdk2*, *Pdk4*, *Slc2a1*, *Slc2a4*) (**i**), lipogenesis (*Gk*, *Screbf1*) and lipolysis (*Lipe*, *Lpl*) (**j**). Data are representative of three independently performed experiments, each performed in technical triplicates. Data represent means ± s.e.m. Asterisks indicate: *, $p<0.05$; **, $p<0.01$ based 2-way ANOVA followed by Bonferroni post-hoc comparison of the individual time-points (**a**-**d**) or student's ttest (**e**-**j**).

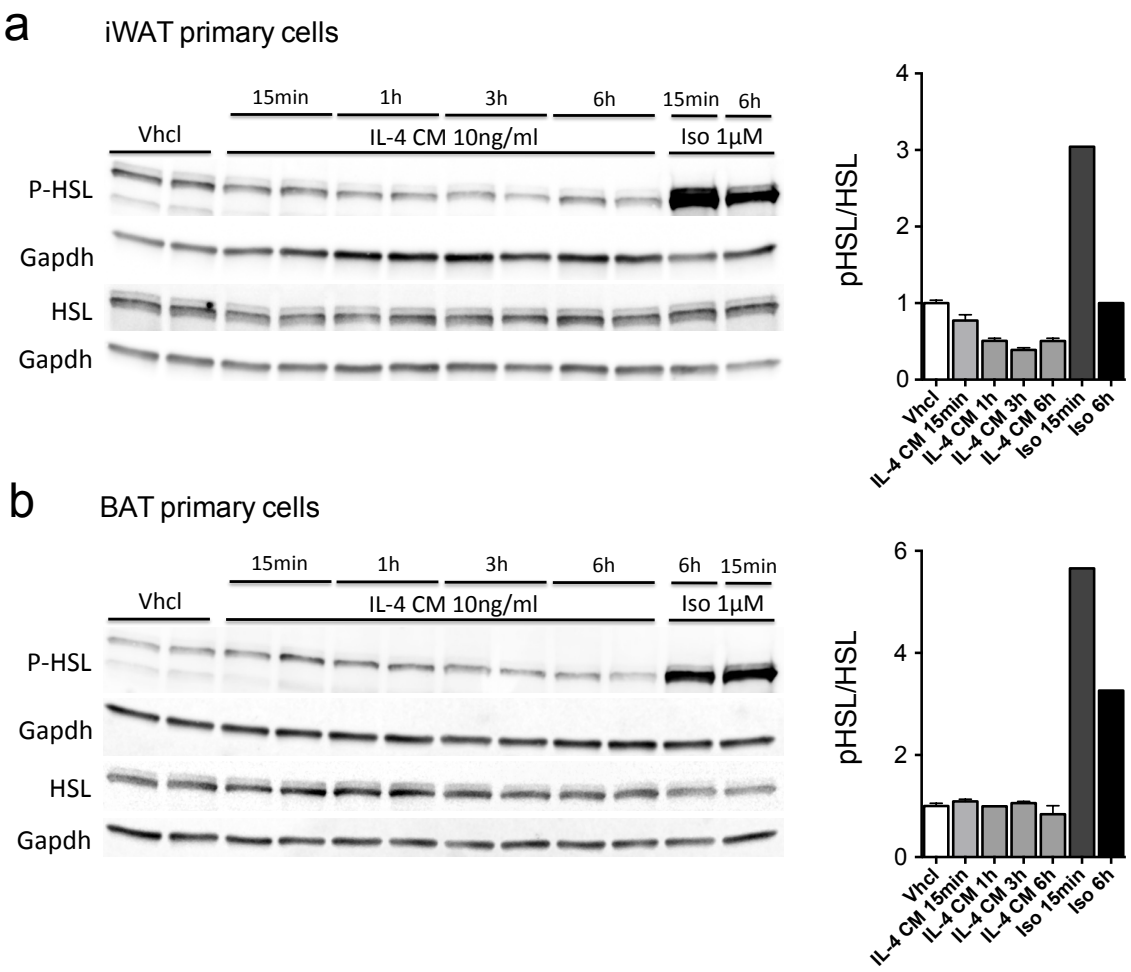

Supplementary Figure 4. Effect of IL-4 on phosphorylation of HSL in BAT and iWAT primary cells.
Western blot analysis of phosphorylated and total HSL of iWAT (**a**) and BAT (**b**) primary cells treated with conditioned media (CM) of IL-4 treated BMDMs (15 min, 30 min, 1 h, 3 h, 6 h) or isoproterenol (Iso) (15 min, 6 h, *n* = 2 technical replicates each treatment). Uncropped Western blot images are shown in Supplementary Figure 12. Data represent means ± s.e.m.

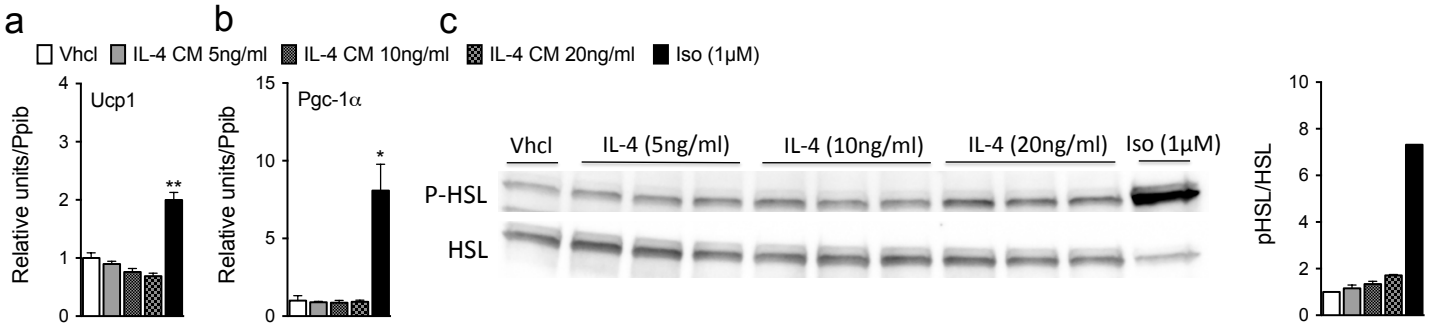

Supplementary Figure 5. Effect of alternatively activated macrophages from the Raw264.7 cell line on thermogenic gene program and HSL activity in primary brown adipocytes.

Expression profile of brown fat-specific markers (*Ucp1, Pgc-1α*) (**a**,**b**) in BAT primary cells treated with conditioned media (CM) from the IL-4 treated Raw264.7 cells or isoproterenol (Iso). Western blot displays protein levels of phosphorylated or total HSL and quantification of the protein levels of p-HSL and HSL (**c**) of 6-d differentiated BAT primary cells treated with CM from IL-4 treated Raw264.7 or Iso (1 μM) for 6 h. Uncropped Western blot images are shown in Supplementary Figure 12. Data are representative for three independently performed experiments, each performed with n = 3 technical replicates. Data represent means ± s.e.m. Asterisks indicate: *, $p<0.05$; **, $p<0.01$ based on 1-way ANOVA followed by Bonferroni-multiple comparison test.

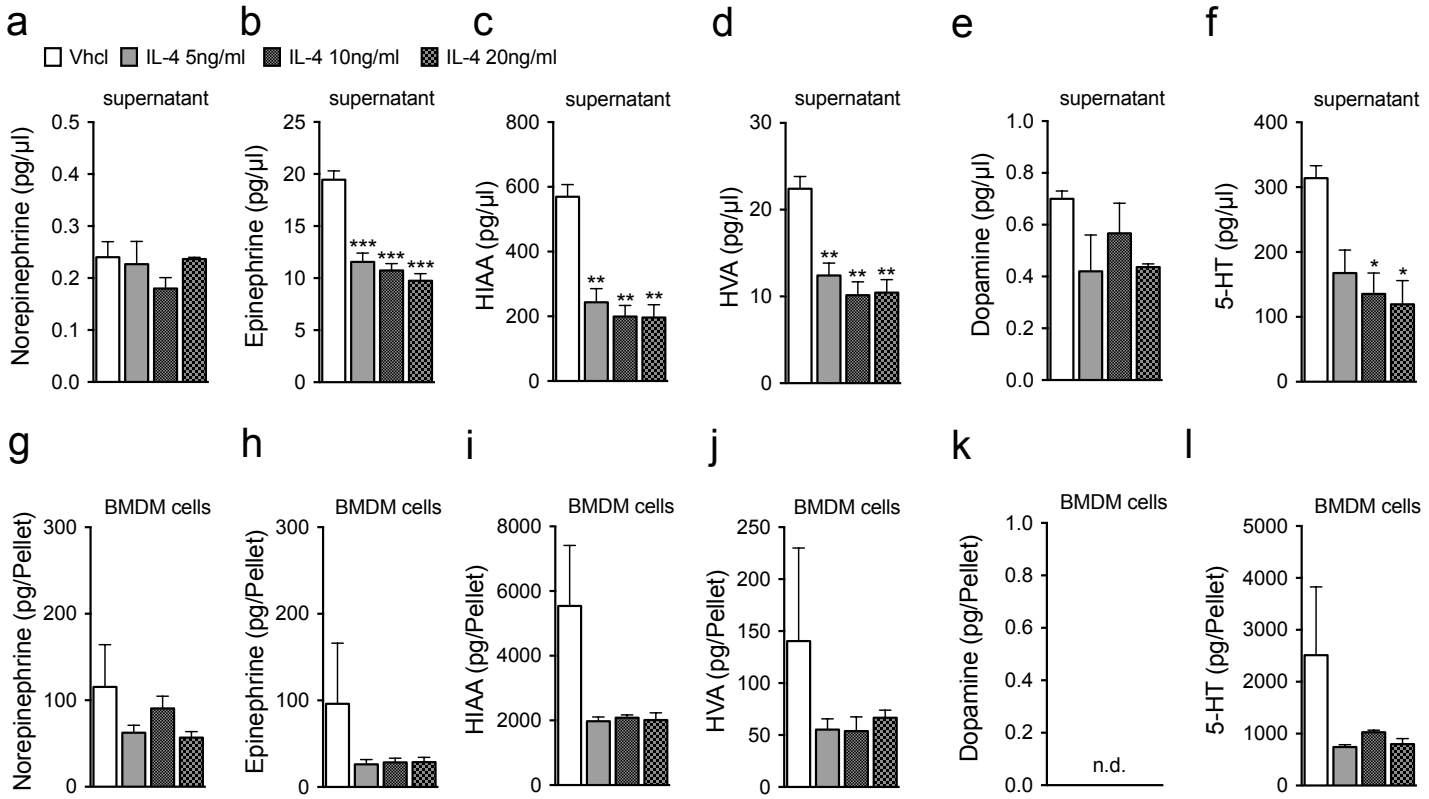

Supplementary Figure 6. Catecholamine production in BMDMs.
HPLC-based measurement of NE, epinephrine, 5-hydroxyindoleacetic acid (5-HIAA), homovanillic acid (HVA), dopamine and 5-hydroxytryptamin (5-HT) in supernatant (**a**-**f**) or cells (**g**-**l**) of vhcl or IL-4 treated BMDMs (*n* = 3 technical replicates each group). Data represent means ± s.e.m. Asterisks indicate: *, p<0.05; **, p<0.01; ***, p<0.001 based on 1-way ANOVA followed by Bonferroni-multiple comparison test.

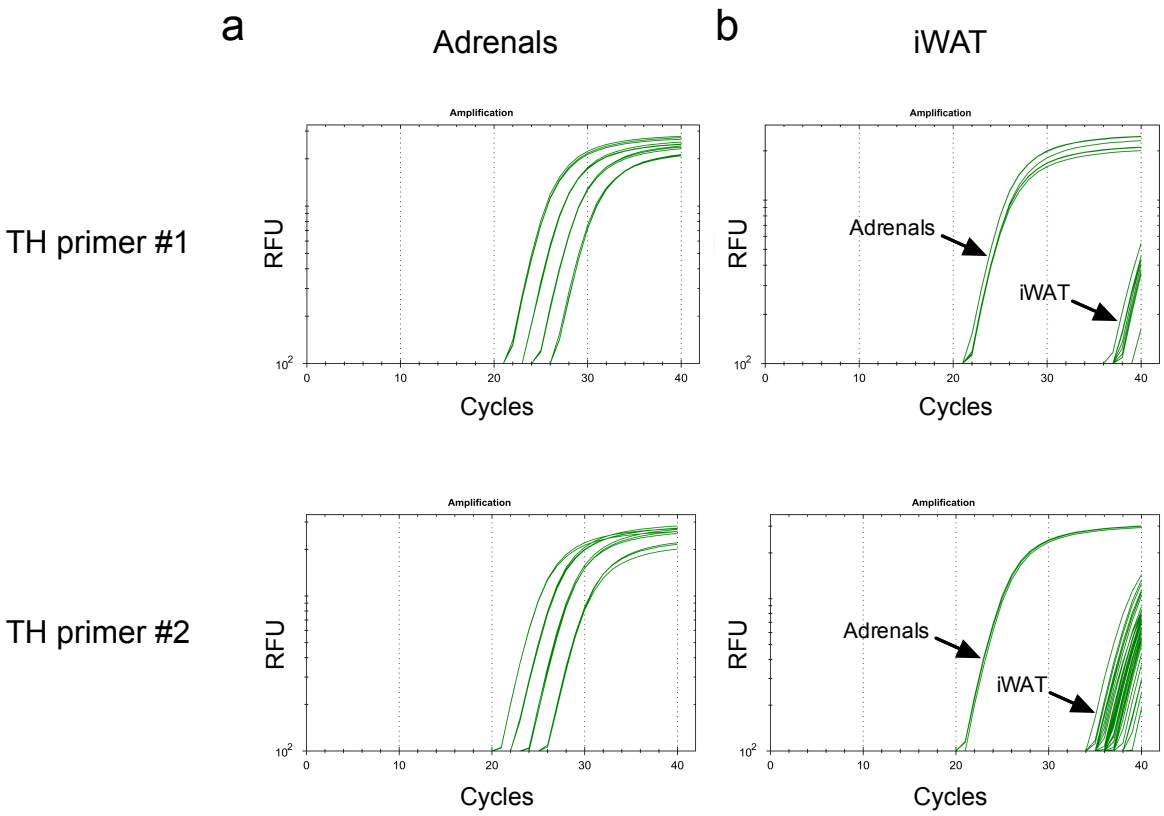

Supplementary Figure 7. TH primer validation
Amplification plots of *TH* gene expression of adrenal (**a**) and iWAT (**b**) extracts from cold-exposed WT mice from 30°C to 4°C. Two different primer pairs (TH primer #1; #2) were validated in *n* = 7 mice. Primer sequences are displayed in Supplementary Table 1.

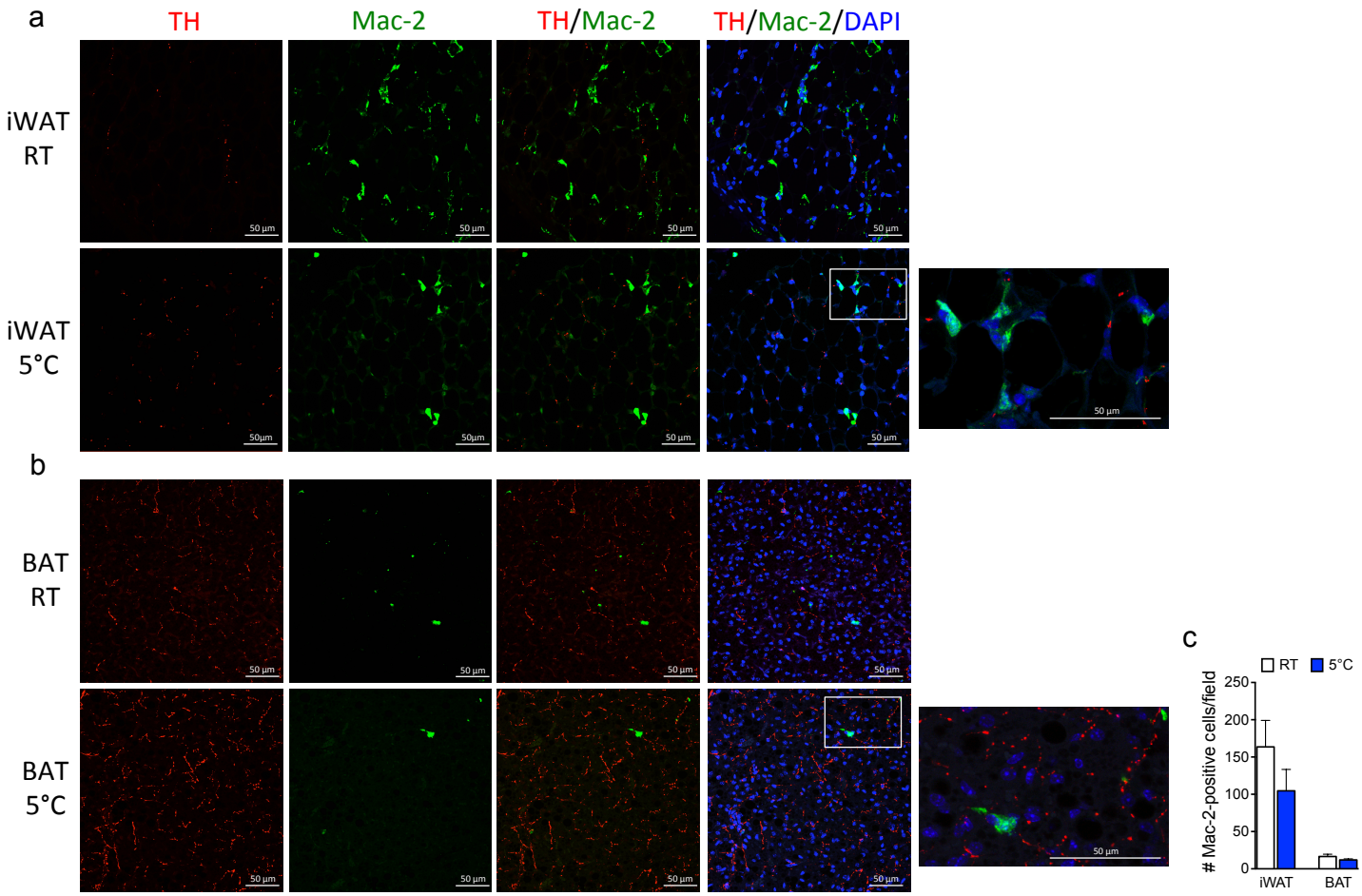

Supplementary Figure 8. TH and Mac-2 co-staining of cold-exposed adipose tissue.
Immunofluorescence of TH and Mac-2 in iWAT (**a**) and BAT (**b**) of room temperature (RT) (top) or 4-h cold-exposed (5°C) (below) C57Bl/6J mice (*n* = 4 mice each group) (scale bar: 50 µm). Quantification of Mac-2-positive cells (number of cells per 20x field) of RT or cold-exposed iWAT and BAT tissues (**c**). Displayed fluorescent images are representative images of *n* = 4 mice per tissue and treatment. Rectangles highlight zoomed-in areas that are displayed right next to it. Data represent means ± s.e.m.

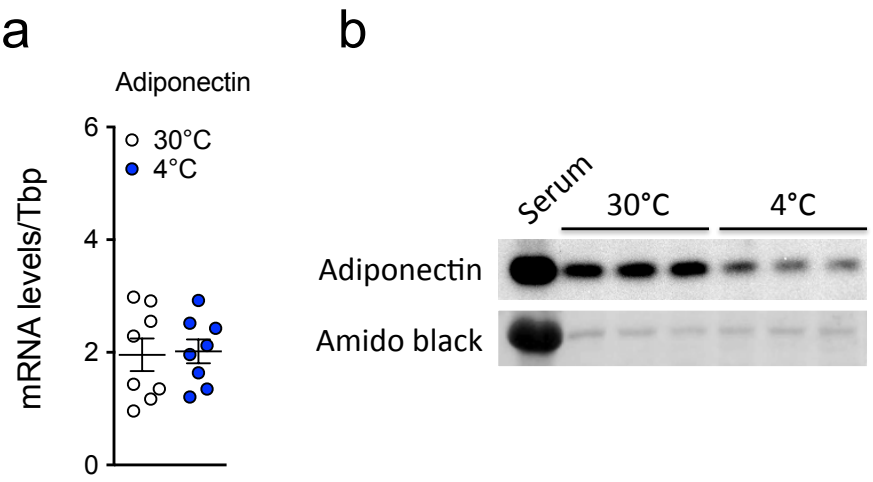

Supplementary Figure 9. Adiponectin expression in iWAT of long-term cold-exposed C57Bl/6 mice.
Gene expression (*n* = 8 mice each group) (**a**) and protein analysis (*n* = 3 mice each group) (**b**) of adiponectin and amido black loading control in iWAT of thermoneutral (30°C) or cold-exposed (4°C) C57Bl/6 mice for 4-5 wks. Uncropped Western blot images are shown in Supplementary Figure 12. Data represent means ± s.e.m.

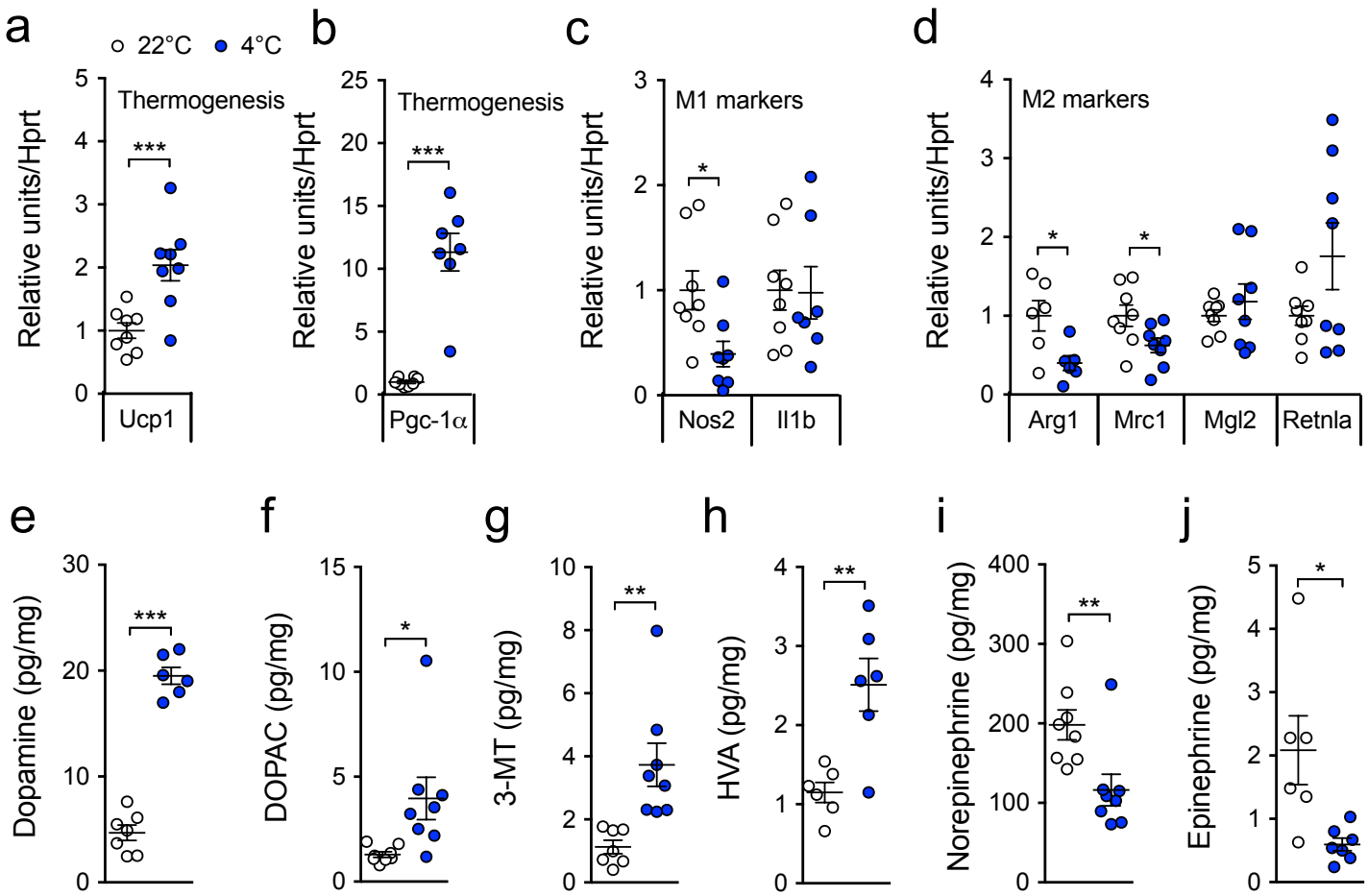

Supplementary Figure 10. Effect of 6-h cold exposure on macrophage content and catecholamine turnover in brown fat.

Gene expression of brown fat-specific markers (*Ucp1, Pgc-1α*) (**a**,**b**), M1 macrophage markers (*Nos1, Il1b*) (**c**) or M2 macrophage markers (*Arg1, Mrc1, Mgl2, Retnla*) (**d**) in BAT from mice housed at 22°C or 4°C for 6 h (*n* = 8 each group). Catecholamines and metabolites, namely dopamine (**e**), 3,4-dihydroxyphenylacetic acid (DOPAC) (**f**), 3-methoxytyramine (3-MT) (**g**), homovanillic acid (HVA) (**h**), NE (**i**) and epinephrine (**j**), were measured in BAT from room temperature or cold-exposed mice (*n* = 8 each group). Data represent means ± s.e.m. Asterisks indicate: *, p<0.05; **, p<0.01; ***, p<0.001 based on student's ttest.

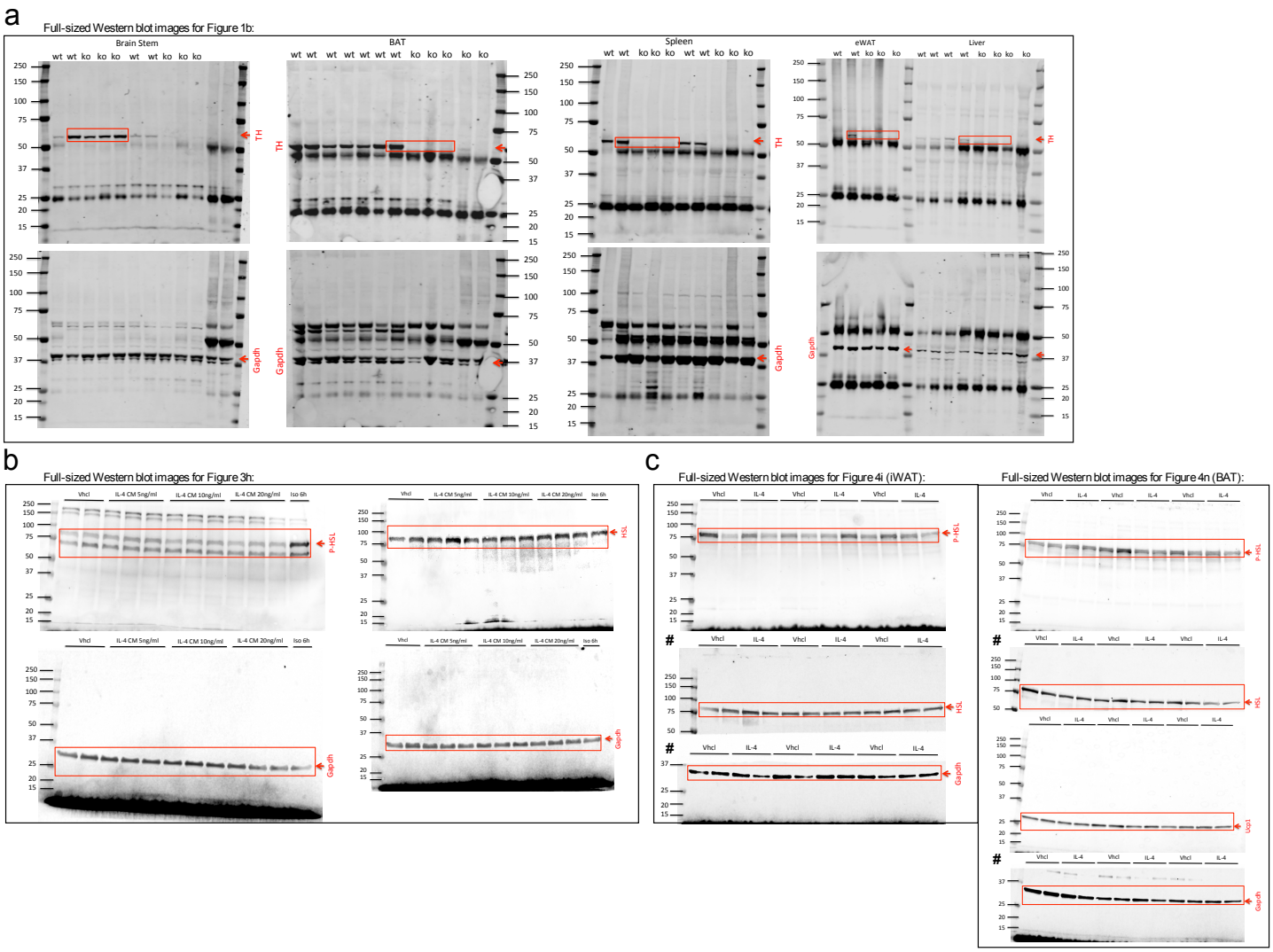

Supplementary Figure 11. Full-scans of Western blots.
Full-sized images of Western blot from Figure 1b (**a**), 3h (**b**) and 4i (**c**). Red boxes highlight areas that were cropped and are displayed in the indicated figures. Red arrows indicate location of the detected protein. Western blot membranes of Figure 4 (indicated with #) were cut out at a size of 50 kDa to detect HSL and Gapdh on separated parts of the membranes.

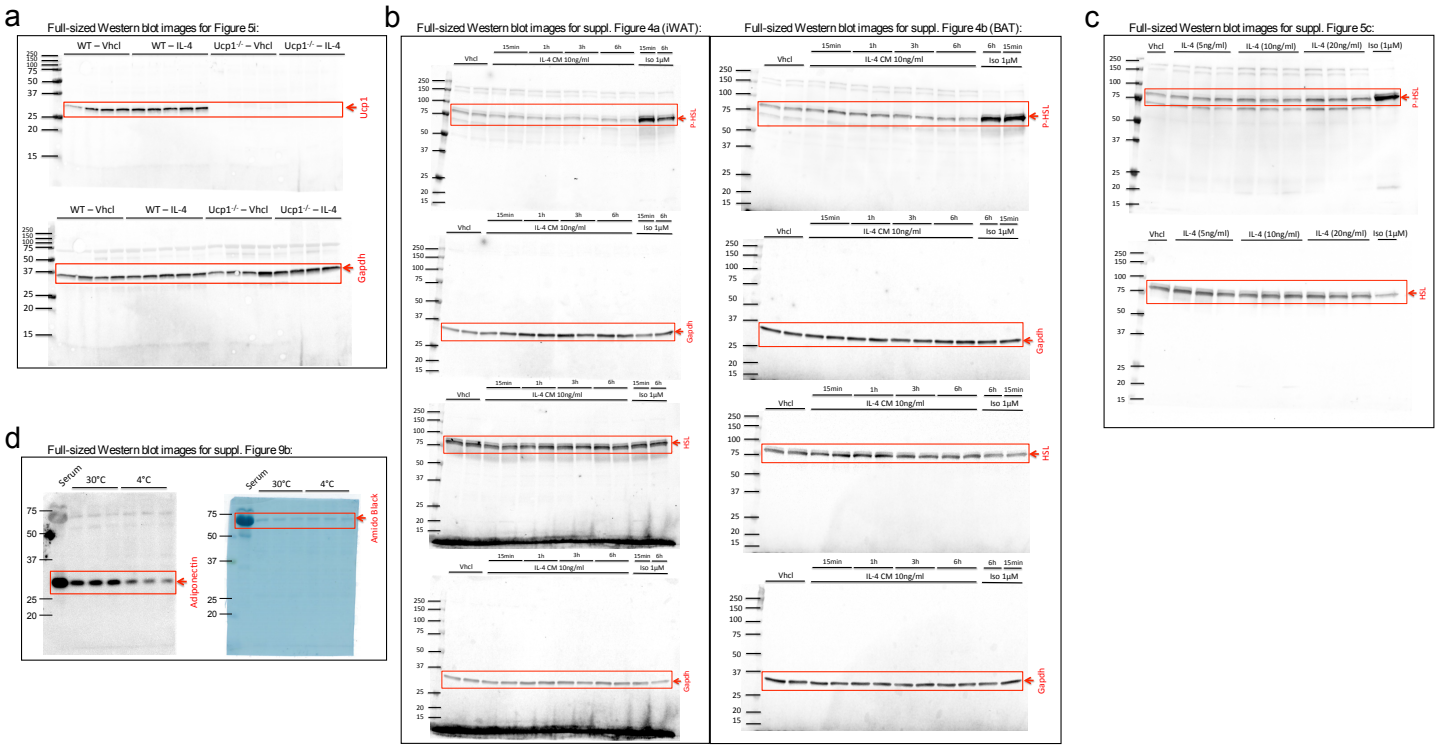

Supplementary Figure 12. Full-scans of Western blots.
Full-sized images of Western blot from Figure 5i (**a**), supplementary Figure 4a,b (**b**), 5c (**c**) and 9b (**d**). Red boxes highlight areas that were cropped and are displayed in the indicated figures. Red arrows indicate location of the detected protein.

Gene	Forward primer (5'-3')	Reverse primer (5'-3')
Dio2	TGCCACCTTCTTGACTTTGC	GGTTCCGGTGCTTCTTAACC
Tnf	AATGGCCTCCCTCTCATCAG	CCCTTGAAGAGAACCTGGGA
Prdm16	CCGCTGTGATGAGTGTGATG	GGACGATCATGTGTTGCTCC
Ppargc1a (Pgc-1α)	AGCCGTGACCACTGACAACGAG	GCTGCATGGTTCTGAGTGCTAAG
Ucp1	GGCCTCTACGACTCAGTCCA	TAAGCCGGCTGAGATCTTGT
Arg1	CTGAGCTTTGATGTCGACGG	TCCTCTGCTGTCTTCCCAAG
Mrc1	TGGATGGATGGGAGCAAAGT	GCTGCTGTTATGTCTCTGGC
Mgl2	TGGAGAGCACAGTGGAGAAG	CGGCAGTACTTGTCAGCTTC
Itgam	TGACCTGGCTTTAGACCCTG	ACCTCTGAGCATCCATAGCC
Adgre1	GAAGCATCCGAGACACACAC	TTGTGGTTCTGAACAGCACG
Cycs	GTTCAGAAGTGTGCCCAGTG	GTCTGCCCTTTCTCCCTTCT
Cox4i1	CTAGAGGGACAGGGACACAC	TGGTTCATCTCTGCGAAGGT
Fasn	AGAGATCCCGAGACGCTTCT	GCTTGGTCCTTTGAAGTCGAAGA
Adipoq	GGTCCTAAGGGTGAGACAGG	AGTCCCGGAATGTTGCAGTA
Fabp4	CAGCGTAAATGGGGATTTGG	CCGCCATCTAGGGTTATGAT
Pparg	TCGCTGATGCACTGCCTATG	GAGAGGTCCACAGAGCTGATT
TH primer 1	GTCTTCCTATGGAGAGCTCCTG	GGCTGGTAGGTTTGATCTTGG
TH primer 2	GCTACCGAGAGGACAGCATT	CACGGGCAGACAGTAGACC
Nos2	CCCCGCTACTACTCCATCAG	CCACTGACACTTCGCACAAA
Il1b	ACTCATTGTGGCTGTGGAGA	TTGTTCATCTCGGAGCCTGT
Retnla	CCCAGGATGCCAACTTTGAA	AGTAGCAGTCATCCCAGCAG
Tbp	GGGAGAATCATGGACCAGAA	GATGGGAATTCCAGGAGTCA
Hprt	AAGCTTGCTGGTGAAAAGGA	TTGCGCTCATCTTAGGCTTT
Ppib	GCATCTATGGTGAGCGCTTC	CTCCACCTTCCGTACCACAT

Supplementary Table 1. List of primer sequences